



Future Climate Change Projections of the Kabul River Basin Using a Multi-model Ensemble of High-Resolution Statistically Downscaled Data

Syed Ahsan Ali Bokhari¹ · Burhan Ahmad¹ · Jahangir Ali² · Shakeel Ahmad² · Haris Mushtaq² · Ghulam Rasul¹

Received: 16 April 2018 / Revised: 10 July 2018 / Accepted: 15 July 2018 / Published online: 9 August 2018
© Springer Nature Switzerland AG 2018

Abstract

In this study, we examined the future climatic changes in the Kabul River basin located in the Hindu Kush Mountain ranges of Pakistan and Afghanistan. We used the latest data set of statistically downscaled CMIP5 Global Climate Models (GCMs), i.e., NASA Earth Exchange Global Daily Downscaled Projections (NEX-GDDP). The data set delivers valuable local scale, high-resolution climate change information for past and future periods (1950–2100) on a daily basis, which is very suitable for exploring future changes in mean and extremes of both temperature and precipitation. Multi-model ensemble derived from NEX-GDDP data effectively produces observed spatial patterns and magnitude of both temperature and precipitation that otherwise cannot be captured with coarse resolution GCMs. For the historical period (1975–2005), NEX-GDDP presented an improved seasonal cycle climatology and correlation coefficient with the observed data set. Future projections using multi-model ensembles indicate a consistent rise in mean temperature over the entire Kabul River Basin, relative to the baseline under RCP4.5 and RCP8.5 emission scenarios. Although the increase in temperature is not uniform across the domain, upper reaches of the basin show annual and seasonal warming of approximately 6.8 °C by the end of the twenty first century under the RCP8.5 scenario. These changes are significant at a 95% confidence level. The rise in summer and winter temperatures may negatively affect the snow accumulation during winter and has the potential to accelerate glacier melting during summers. Projections of future precipitation under both scenarios show an overall decrease in mean precipitation, particularly under the RCP8.5 scenario.

Keywords Kabul River Basin · PDFs · CMIP5 · Future projections · NEX-GDDP

1 Introduction

Climate change is the greatest challenge that the world is facing today. Its impacts on water resources especially can be quite diverse and uncertain. During the last century, a 1–2 °C increase in global mean temperature was observed, which has far-reaching consequences such as accelerated glacier melting and increases in the frequency of extreme weather events (Cruz et al. 2007). The Hindu Kush–Karakoram–Himalaya (HKKH) region has the highest density of glaciers outside the Poles. They feed many rivers; amongst them are seven of Asia's greatest rivers—Brahmaputra,

Ganges, Huang Ho, Indus, Mekong, Salween, and the Yangtze. The life of more than two and half million people is highly affected by any changes in these rivers. HKKH region is termed as the most tenuous ecological zone regarding climate change resilience (Jianchu et al. 2007; Singh et al. 2011). Different climate conditions co-exist in these complex mountain ranges, due to the influence of multiple circulation systems and several climate feedbacks of atmosphere, cryosphere, and hydrosphere, thus making the region highly vulnerable to climate change-related impacts (Palazzi et al. 2013). By the end of the twenty first century, warming over the HKKH is projected to remain higher than the global mean temperature average (Iqbal et al. 2018). Runoff due to snowmelt from the mountain regions is important for a sustained water supply (Nestler et al. 2014). Changing climate is accompanied with a significant change in the steam flow of regional river basins such as Kabul River particularly due to the presence of snow- and ice-based freshwater resources

✉ Syed Ahsan Ali Bokhari
Ahsan.pmd@gmail.com

¹ Pakistan Meteorological Department, Islamabad, Pakistan

² LEAD Pakistan, Islamabad, Pakistan

(Abbaspour 2015; Sidiqi et al. 2018). The presence of climate change-related vulnerabilities poses a serious threat to the socio-economic development of the population that is dependent on the water resources of Kabul River.

Global Climate Models (GCMs) are being widely used by the scientific community in the studies of past climates, and to project the future climate under different socio-economic and Greenhouse Gas (GHG) emission scenarios (Almazroui et al. 2012; Annamalai et al. 2007; Taylor et al. 2012). The coarse resolution of GCMs, lacking to represent the detailed topography and small-scale process, results in large biases for both temperature and precipitation (Leung et al. 2003; Suzuki-Parker 2012). To overcome this limitation of GCMs, several downscaling techniques have been developed which include both statistical and dynamical procedures (Ekström et al. 2015; Murphy 1999). Statistical downscaling is based on the statistical relationships between the coarse GCMs and finely observed data and is computationally straightforward for obtaining high-resolution climate projections. Although statistical downscaling can be a computationally efficient alternative to dynamic downscaling, it relies on an assumption that the empirical relationship identified for the current climate will hold for future climate scenarios (Wilby et al. 2004). The dynamical downscaling involves the simulation of more realistic physical processes at a finer scale using regional climate models (RCMs). RCMs are provided with the lateral boundary conditions from coarse resolution GCMs output. During the recent 2 decades, many RCMs have been developed with an improved capability to resolve physical processes. They are being widely used in regional-scale climate studies including assessments of past climate and future climate projections (Giorgi et al. 2012; Iqbal et al. 2016; Pal et al. 2007; Parajka et al. 2010; Rummukainen 2010). Despite being the best available tool, there are uncertainties associated with RCMs projections due to the systematic biases of the driving GCMs and internal variability and sensitivity of the RCM to numerical schemes and resolution-dependent processes (Bachner et al. 2008; Mehmood et al. 2009; Pfeiffer and Zängl 2011; Syed et al. 2009; Syed et al. 2014). Therefore, downscaled GCMs with bias corrections produce more accurate data at a fine resolution for future projections (Ficklin et al. 2016). For robustness and statistical significance of the results, ensemble and multi-modeling techniques are often applied (Knutti 2008; Madadgar and Moradkhani 2014). Although there exists a large inter-model variance in ensembles, varying physical schemes among single ensemble members can provide a more reasonable representation of the physical processes attributed to climate variability and change (Almazroui et al. 2012; Tebaldi and Knutti 2007; Vidale et al. 2003). Immerzeel et al. (2012) applied an ensemble of statistically downscaled GCMs to study the future water cycle variability in a glacierized catchment in Nepal. A multi-model ensemble of statistically

downscaled GCMs showed very good performance in capturing the precipitation and temperature climatology in the Indus River Basin (Su et al. 2016).

Palazzi et al. (2013) analyzed long-term historical (1950–2009) trends of precipitation from a range of observed and reanalysis data sets and found no statistical significance trend for winter in the Hindu Kush–Karakoram (HKK) region. Moreover, they also analyzed future projections of whole HKKH region using eight ensemble members of the EC-EARTH model of CMIP5 family under RCP4.5 and RCP8.5. The future projections show a statistically significant increase in winter precipitation of around 0.4–0.7 mm/day over the HKK region under both scenarios, while no significant trend is shown under RCP4.5 scenario for summer. Palazzi et al. (2015) presented an evaluation for past climatology and trends (1901–2005) of precipitation in the HKKH region as reproduced by 32 GCMs of CMIP5 family. They found a large inter-model disagreement of seasonal and annual patterns and statistics for all the 32 GCMs, which make it difficult to rely on a single model output. The future projections under the RCP8.5 scenario indicate a wetter summer during twenty first century for HKK area, while winter precipitation shows no significant change. Hasson et al. (2013) assessed the performance of PCMDI/CMIP3 GCMs in simulating the hydrological cycle over four major river basins in South and Southeast Asia (Indus, Ganged, Brahmaputra, and the Mekong). For twentieth century climate (1961–2000), 4 out of 13 models show water deficit in the Indus basin mainly due to underestimation of observed precipitation minus evaporation ($P - E$). The poor performance of those models is attributed to an underestimation of observed precipitation. The future projections (2061–2100) under the SRES A1B scenario do not indicate any change in inter-annual variability of $P - E$ during the twenty first century. There is disagreement among different models in estimating the future water balance for Indus basin, since models feature inconsistent magnitude of change in precipitation and evaporation. Hasson et al. (2016) reviewed the skill of 30 CMIP5 models in simulating the seasonal cycle of precipitation for the same river basins. They assessed the model's performance by virtue of their ability in accurately estimating the timing of the monsoon onset and its seasonality during the active phase. None of the models or the multi-model ensemble performed best for the chosen skill metrics. One-third of the models were not able to simulate the observed patterns and timing of monsoon precipitation over the Indus basin. Future projections suggest a westward extension of monsoon regime over Pakistan. Rajbhandari et al. (2015) performed high-resolution (50 km × 50 km) simulations of Indus Basin's past and future climates using RCM (PRECIS). The model showed a good agreement with the observed data in capturing the topography variations and seasonal cycle of precipitation with

the presence of quantitative biases. The model projections under the A1B scenario indicate a decrease in winter precipitation over the Upper Indus Basin. Upper parts of the Indus Basin show increased warming in the future compared to the lower parts, which is more pronounced in winter. A multi-model ensemble of 21 CMIP5 GCMs shows a consistent warming in the Upper Indus Basin during the twenty first century under three emission scenarios, i.e., RCP2.6, RCP4.5, and RCP8.5 (Su et al. 2016). Monsoon precipitation is projected to increase over the Indus Basin, while models show a decrease in winter precipitation. A recent study published by Hasson et al. (2018) assessed the robustness of the climate change signal for Jhelum, Kabul, and UIB as simulated by high-resolution dynamical models within the framework of Coordinated Regional Climate Downscaling Experiment for South Asia (CX-SA). The model's skill was evaluated in terms of its ability to reproduce past climatology of temperature and precipitation from 1971–2005 and the seasonal cycle of precipitation. The findings show a low fidelity of the CX-SA data set based on applied statistical metrics and high, cold, and wet biases and an inaccurate seasonal cycle of precipitation that is notably consistent with its driving CMIP5 models. These results highlight the uncertainty of future projections of precipitation and temperature due to the inter-model disagreements of CX-SA and CMIP5 models for the historical period. The contradictory precipitation projections for this basin make water availability in the Upper Indus Basin highly uncertain and require further research (Lutz et al. 2016). No study has specifically focused on the prediction of the future climate of the Kabul River Basin using bias-corrected and high-resolution climate

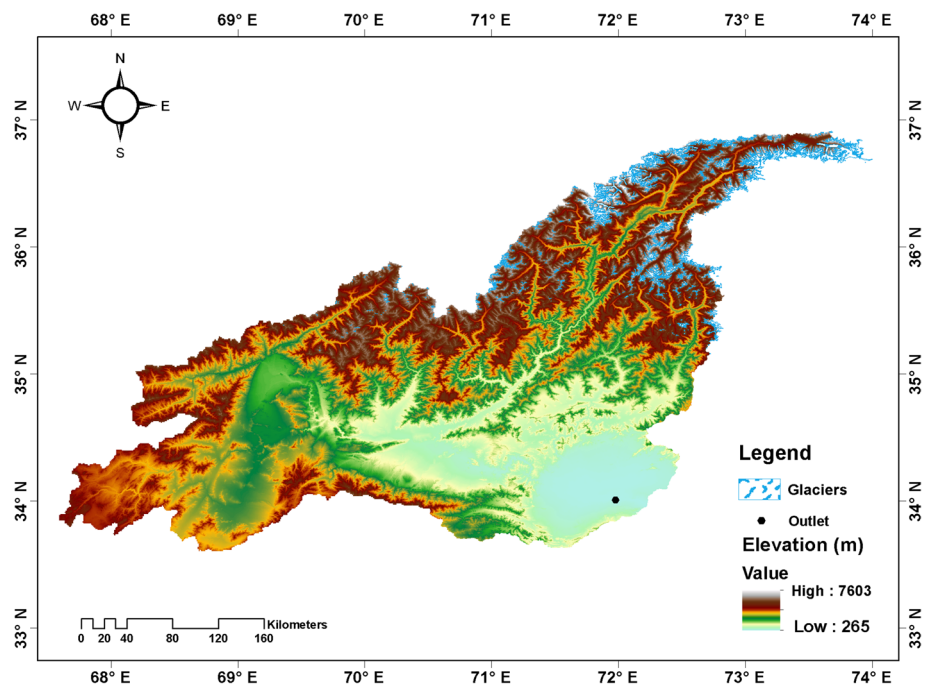
change projections. The objective of this study is to provide a robust assessment of the present-day climate and its future changes under two emission scenarios (RCP4.5 and RCP8.5) using statistically downscaled and bias-corrected projections of GCMs of the CMIP5. This study, based on 21 downscaled GCMs and two scenarios (RCP4.5 and RCP8.5) of CMIP5 family, is the most up-to-date and is suitable for studying the impact of climate change on water resources of a shared basin under both moderate (RCP4.5) and extreme (RCP8.5) emissions' scenario. The results of this study will form an important basis for the estimation of changes in the hydrological cycle of the basin and inform decision makers and water policy experts to devise future interventions in light of these climate change projections.

2 Study Area, Models, Data, and Methodology

2.1 Study Area

The Kabul River Basin (hereafter, KRB) is an upland enveloped by mountains stretching through the northwestern part of Pakistan to the eastern central part of Afghanistan (Fig. 1). The Kabul River originates from the Hindu Kush Mountains and is one of the major rivers in Afghanistan with a high population density (UNFPA n.d.). The Basin covers an area of about 92,000 km² and splits into five sub-basins: (1) The Paghman river, which merges into the Basin from the west where it evolves into a tributary of the KRB and eventually merges into an Indus catchment over the Pakistan

Fig. 1 Boundaries of Kabul River Basin and elevation in meters. Glaciers are marked in blue and white shade. Black dot shows the location of outlet river gauging station (Data Source: Jarvis et al. 2008; Bajracharya and Shrestha 2011)



side of the Basin; (2) The Logar river, which merges into the Basin from the south and discharges therein; (3) The Kunar river, originating from the Chitral Valley in Pakistan, entering Afghanistan through Kunar and rerouting towards Pakistan after flowing up to Jalalabad province in Afghanistan; (4) The Salang, Ghorband, and Panjshir rivers, forming the Ghorband–Panjshir watershed; (5) The Alishang and Alinigar rivers, converging at Surobi (Hassanyar et al. 2017; Lashkaripour and Hussaini 2007). The Kabul River, with its five tributaries, makes around 26% of the available water resources in Afghanistan, having a mean annual stream flow of about 24 billion cubic meters (King and Sturtewagen 2010), and irrigates 66,748 km² of land (FAO 2016). Around 72% of the total runoff is generated by seasonal snowmelt (Sidiqi et al. 2018). An estimated 9 million people living in Afghanistan and Pakistan share the water resources of KRB. According to Bajracharya and Shrestha (2011), there are around 1600 glaciers located in the Kabul basin, with the highest and largest concentration in the Kunar and Swat sub-basins. The climate in the basin is semi-arid and robustly continental. The maximum precipitation observed during the winter months averages 110 mm. The highest maximum temperature is observed in July, with an average value of approximately 28 °C, while an average minimum temperature during winter is about –6 °C (Hassanyar et al. 2017). There is a high variation of received precipitation throughout the year due to the complex terrain. Historic data records show that the highest mean annual precipitation of more than 1600 was received in the northern parts of the basin (Lashkaripour and Hussaini 2007). Approximately, all the precipitation in the basin falls during the winter season. The precipitation is mostly “snow precipitation,” which is reserved over the mountains to recharge the rivers in the melt season. Rivers dehydrate when the snow has completely melted. Hence, there is no continuous water supply available in the rivers flowing within the KRB. Water supply from snow or ice melt represents a major contribution to discharge during the summer months.

2.2 Data

To examine future changes in temperature and precipitation of the KRB, a high-resolution NASA Earth Exchange Global Daily Downscaled Projections (NEX-GDDP) data set is used in this study. NEX-GDDP was recently made available to the global scientific community and is particularly aimed at providing past and future climate change information at the finest possible scale (Thrasher et al. 2012). Therefore, the choice of the data set in this study is related to its significance in providing researchers and policymakers with the required information about the impacts of climate change at a city and basin scale. NEX-GDDP is the output of CMIP5 21 GCMs downscaled at 0.25° spatial resolution

and available as daily data projections from 1950–2100. The downscaling method adopted in development of this data set is Bias Correction and Spatial Disaggregation (BCSD) which is a regression-based statistical technique applied to improve the efficiency of low-resolution GCMs for removing local biases (Maurer and Hidalgo 2008; Thrasher et al. 2012, 2013; Wood et al. 2004). This downscaling approach is a two-step process. It starts with a comparison of GCMs historical (1950–2005) simulation against observations to compute biases or differences in slope, mean, and variance. The reference observation data used in this step are 0.25° daily maximum temperature, daily minimum temperature, and daily precipitation data from Global Meteorological Forcing Data set (GMFD) for Land Surface Modeling. The GMFD data set is a merger of observations with NCEP/NCAR reanalysis and developed by the Terrestrial Hydrology Research Group at Princeton University (Sheffield et al. 2006). The bias is then applied to the GCMs future projections (2006–2100) data by generating cumulative distribution function (CDF) and mapping quantiles of both historical and GCMs values. In the second step, spatial disaggregation is performed to interpolate the bias-corrected GCMs data to the high resolution (0.25°) of the observations data set (Wood et al. 2002, 2004). The interpolation is not just linear. The process is a multi-step approach to preserve the finer local-scale details of the GMFD data set. The globally downscaled daily data set is available through the NASA Climate Model Data Service (CDS) by subsetting the study region (<https://cds.nccs.nasa.gov/nex-gddp>). Table 1 contains names of 21 GCMs, included in the NEX-GDDP data set. To project the state of the future climate, a multi-model ensemble of 21 downscaled models is computed.

The observed data set used for evaluation of NEX-GDDP data and raw GCMs is ANUSPLIN-generated gridded climate surface obtained from CSIRO, Australia (Hutchinson and Xu 2013). The data for maximum temperature, minimum temperature and precipitation are interpolated at 1 km from on-ground meteorological stations using ANUSPLIN v4.5. ANUSPLIN applies thin-plate smoothing splines for

Table 1 CMIP5 models downscaled in the NEX-GDDP data set (Source: Thrasher et al. 2012)

1	ACCESS1-0	12	INMCM4
2	BCC-CSM1-1	13	IPSL-CM5A-LR
3	BNU-ESM	14	IPSL-CM5A-MR
4	CanESM2	15	MIROC-ESM
5	CCSM4	16	MIROC-ESM-CHEM
6	CESM1-BGC	17	MIROC5
7	CNRM-CM5	18	MPI-ESM-LR
8	CSIRO-MK3-6-0	19	MPI-ESM-MR
9	GFDL-CM3	20	MRI-CGCM3
10	GFDL-ESM2G	21	NorESM1-M

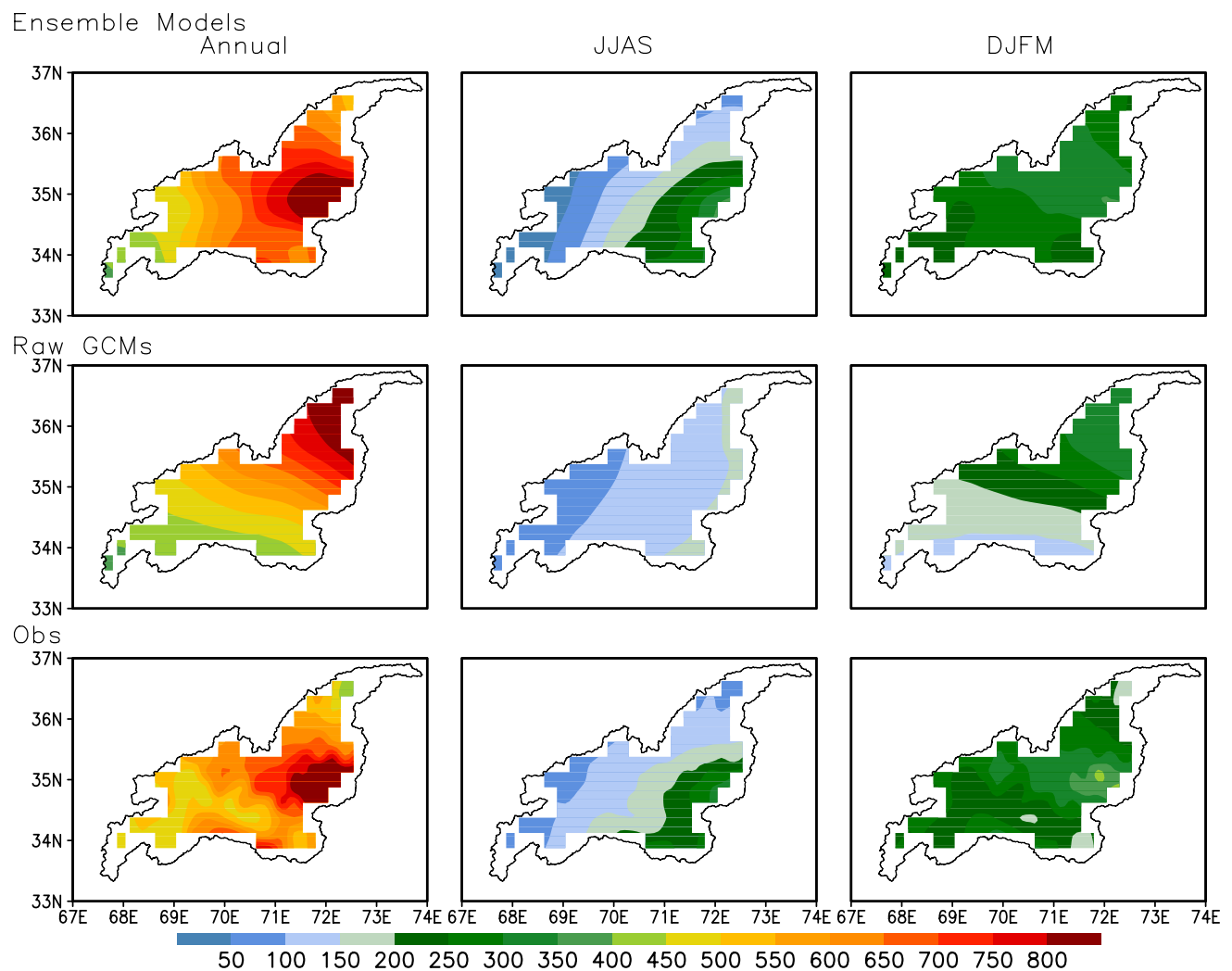


Fig. 2 Historical climatology of mean precipitation (mm) (1975–2005) as produced by NEX-GDDP multi-model ensemble (top row), raw GCMs ensemble (middle row), and observed (bottom row)

data interpolation of on-ground meteorological data of Pakistan Meteorological Department (PMD) to a fine grid ($0.01 \times 0.01^\circ$) and provides a platform for statistical analysis of multivariate data and estimation of spatial errors (Chen et al. 2016). The performance of ANUSPLIN 1 km data for Upper Indus Basin (UIB) and at catchment scale has been compared with APHRODITE and Watch data sets during 1979–2007. Although complete results are not presented by Chen et al. (2016), the PMD observation-based data have shown the best performances due to the highest number of in situ observations. The climate data set is particularly recommended for hydrological modeling. Monthly data for temperature and precipitation for the same GCMs, which were downscaled in NEX-GDDP data set, were downloaded from ESGF portal (<https://esgf-node.llnl.gov/projects/cmip5/>) for the historical period (1950–2005) for comparison and evaluation. The resolution of raw models differs from each

other. However, for the purpose of evaluation, all models were regridded to the common grid of NEX-GDDP data. Out of 21 GCMs included in the NEX-GDDP data set, four GCMs, namely BCC-CSM1-1, BNU-ESM, CESM1-BGC, and CSIRO-MK3-6-0, were not present on ESGF and were, therefore, excluded from a multi-model ensemble of NEX-GDDP and raw GCMs.

2.3 Methodology

To evaluate the performance of the NEX-GDDP data set for the study region, the results of seasonal and annual climatology for both temperature and precipitation were compared with raw GCMs as well as with observed climatology (1975–2005). For spatial comparison with NEX-GDDP, the gridded observations data were interpolated at $0.25^\circ \times 0.25^\circ$ grid resolution. For analysis and discussion of results, the

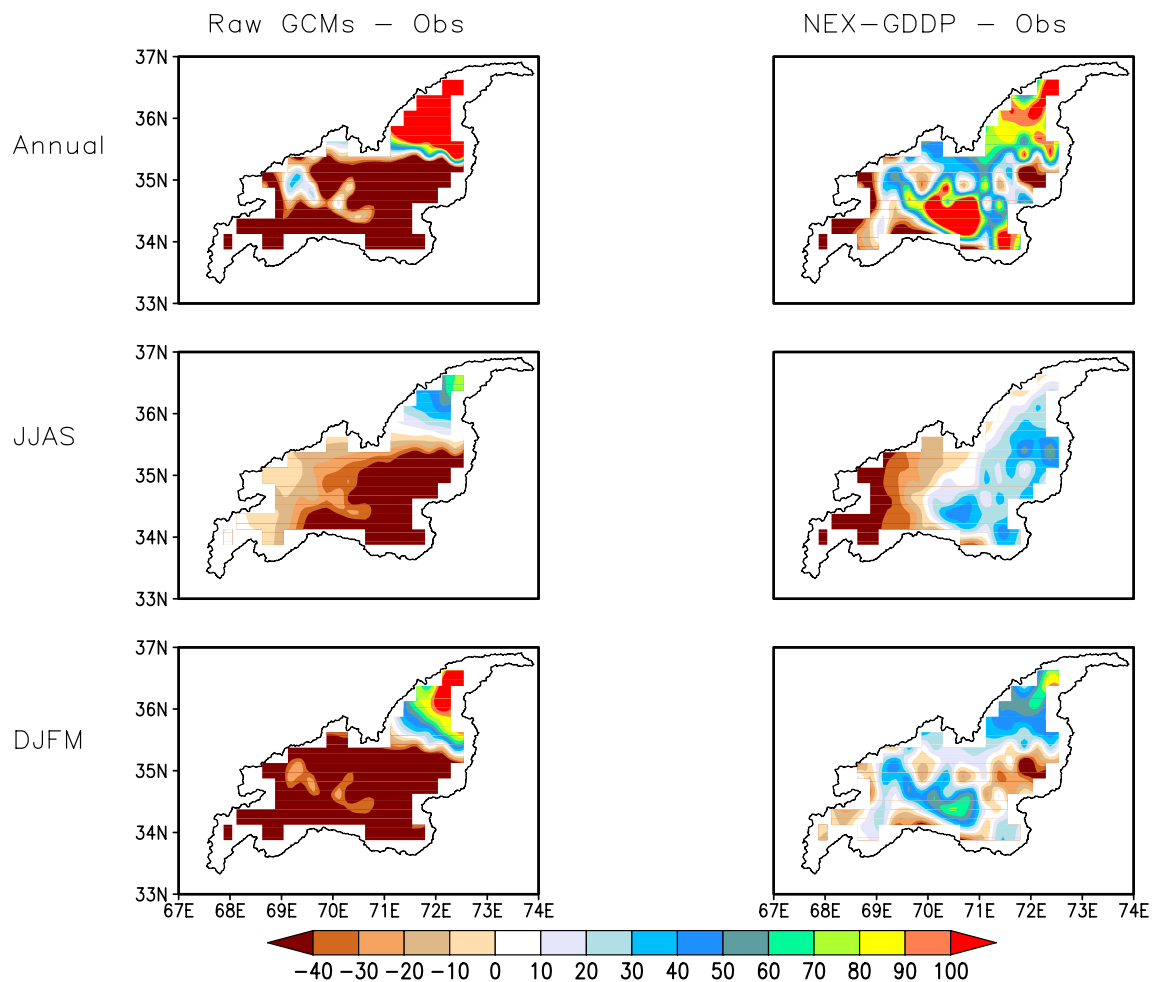


Fig. 3 Geographical distributions of bias for mean precipitation (mm) and between the raw GCMs' multi-model ensemble and observation (ANUSPLIN) and NEX-GDDP multi-model ensemble from 1975 to 2005

baseline and future climates are defined as 30-year time slices: the historical period from 1975–2005; the near-term future from 2010–2039 (hereafter, near-term); the mid-term future from 2040–2069 (hereafter, mid-term); and the end of the century (EOC) future from 2070–2099 (hereafter, EOC). Projected changes of temperature and precipitation are analyzed on both annual and seasonal basis, i.e., winter (December, January, February, and March; hereafter DJFM) and summer (June, July, August, and September; hereafter JJAS). For a more robust evaluation, the efficiency of the data set was measured by examining statistical metrics using the Taylor diagram (Taylor 2001). The diagram provides a summary of the model's performance in simulating the spatial patterns of different variables in terms of their Pearson correlation, the standard deviation (SD), and root-mean-square difference (RMSD). The correlation is shown along the circular axis which improves as a model is located close to observation on the x -axis. Normalized standard deviation (SD) of observation is taken as 1, while the SD of each

model is shown in terms of its distance from the observation. Similarly, RMSD of each model is shown as the distance from the observations on the x -axis. The Taylor diagram is computed for the entire KRB by evaluating all 21 models of NEX-GDDP data for both temperature and precipitation against the observed data of ANUSPLIN.

Probable shifts in the means, the standard deviations, the skewness, and the kurtosis of the normal frequency distribution of both temperature and precipitation are analyzed over the entire Kabul Basin using Probability Density Functions (PDFs). The PDFs respond to shifts in the distributions on means and extremes. They have the ability to depict different changes in distributions between the present and future climate and their reactions on the mean and extreme values of the distributions. They can show the effects of a simple shift of the complete distribution approaching a warmer climate. They can illustrate the effects of escalation in variability with no shift in the mean. Moreover, the effects of a reshaped distribution, e.g., a change in symmetry of the

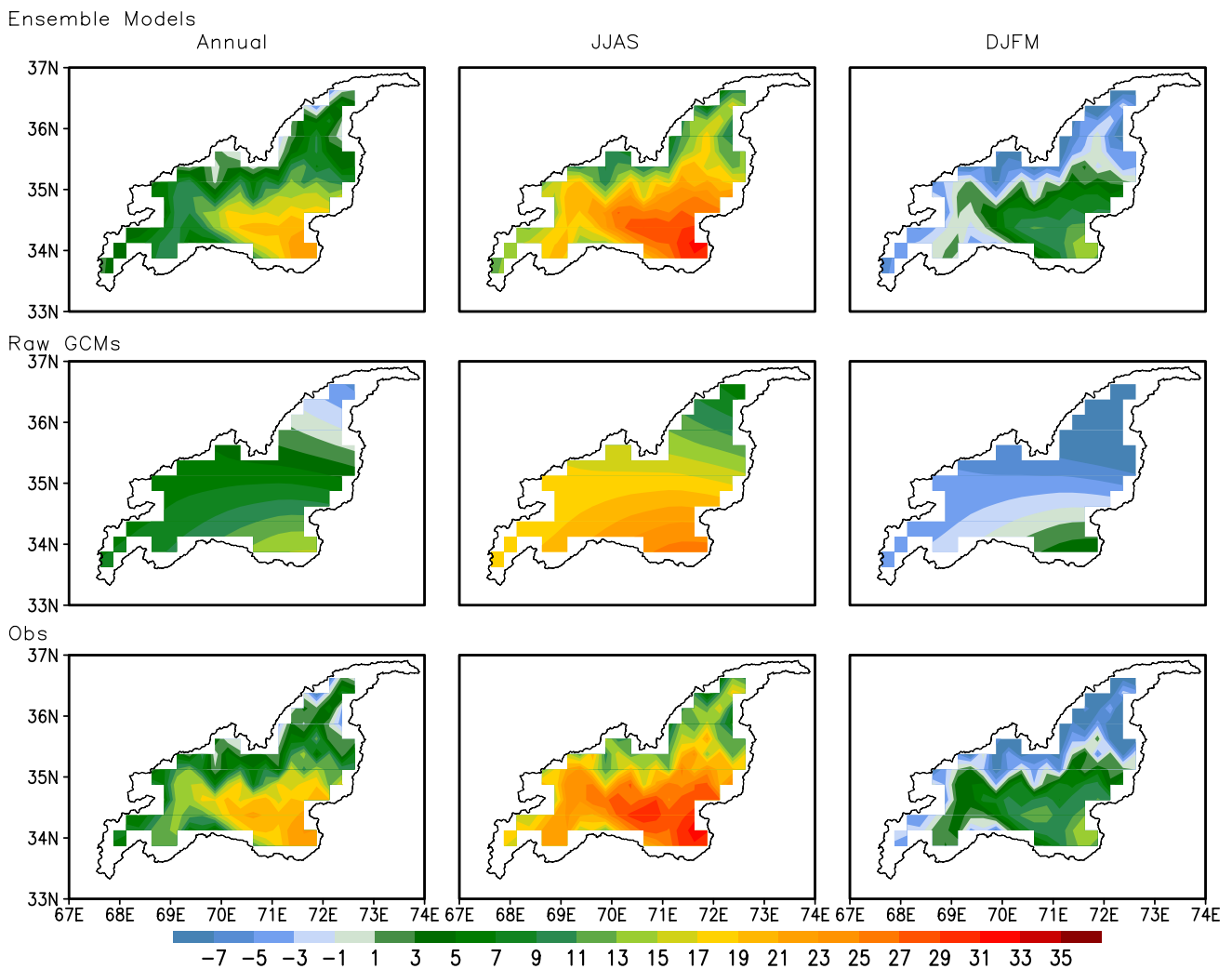


Fig. 4 Historical climatology of mean temperature (°C) (1975–2005) as produced by NEX-GDDP multi-model ensemble (top row), raw GCMs ensemble (middle row), and observed (bottom row)

distribution, can also be identified based on the shapes of a PDF. The outcomes of time-dependent PDFs indicate a shift of the variables towards higher/lower values in the projected period in contrast to the recent/older period with corresponding homogeneous/heterogeneous changes in the variance.

3 Results and Discussion

3.1 Historical Climate

Figure 2 shows historical climatology of precipitation for annual, JJAS, and DJFM from raw CMIP5 GCMs, compared to NEX-GDDP and to observations (ANUSPLIN). As evident in Fig. 2 (top row), NEX-GDDP is showing a very good match with observations in terms of both spatial patterns

and the mean value of the precipitation on annual and seasonal scales. However, the precipitation varies greatly across the domain and annual precipitation ranges from 350 to 800 mm. During the summer season, annual precipitation is lowest on the Afghanistan side of the basin, ranging between 50 and 100 mm and gradually increasing towards the eastern parts of the basin up to 600 mm. Winter precipitation is mostly between 200 and 450 mm, reflecting both seasonal snow and rainfall brought by western disturbances (Yadav et al. 2010). As evident, NEX-GDDP has outperformed raw-GCM is simulating the amount and spatial extent of both summer and winter precipitation when compared with the observed data set. The spatial differences are shown in terms of biases between raw GCMs and ANUSPLIN, as well as between NEX-GDDP and ANUSPLIN (see Fig. 3). NEX-GDDP remarkably reduced the overestimation of precipitation by raw GCMs over the higher northeast parts of KRB,

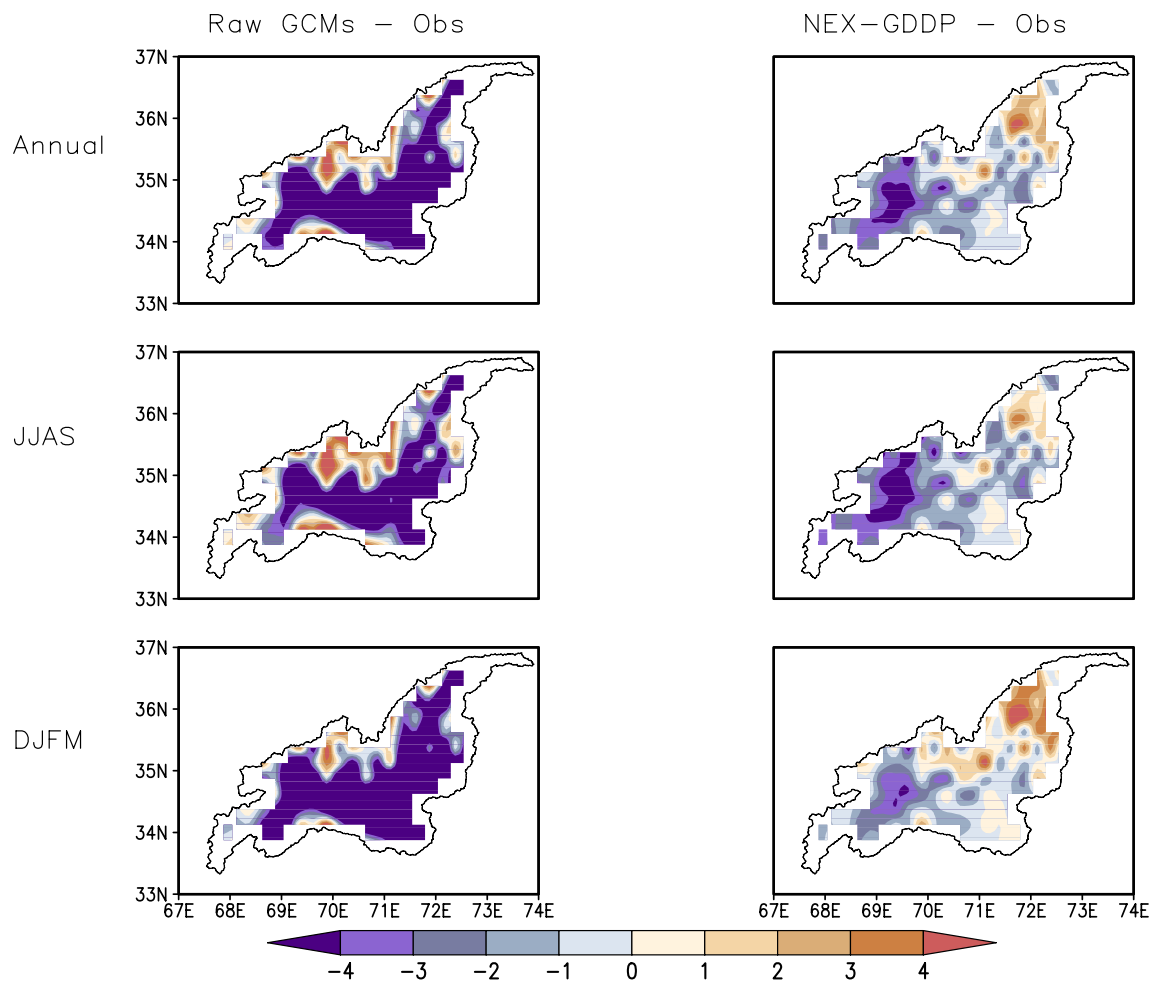


Fig. 5 Geographical distributions of bias for mean temperature ($^{\circ}\text{C}$) and between the raw GCMs' multi-model ensemble and observation (ANUSPLIN) and NEX-GDDP multi-model ensemble from 1975 to 2005

which is mostly snow-covered and glaciated. While raw GCMs not only underestimated the amount of precipitation, a dry bias of more than 40 mm, they also failed to capture the observed spatial variation in lower parts of KRB, which is within the extent of monsoon currents during summer. Similarly, raw GCMs underestimated winter precipitation (dry bias) mostly over the western parts of the KRB, while NEX-GDDP again showed very good spatial match and small biases (Figs. 2, 3). In the high elevation areas, CMIP5 GCMs failed to catch the local-scale variation in temperature, which is accurately represented by NEX-GDDP and consistent with observations.

Historical climatology of the mean temperature for KRB from the NEX-GDDP ensemble models, ensemble raw GCMs, and ANUSPLIN is shown in Fig. 4. Again, NEX-GDDP showed a close spatial pattern and an amplitude of mean temperature with the observations on both an annual and seasonal basis. Mean annual temperatures range between -3 and 21 $^{\circ}\text{C}$. The northern parts of KRB

show relatively low mean temperatures due to high elevation, snow receiving peaks. During the summer season, the temperature mostly ranges between 15 and 33 $^{\circ}\text{C}$. During winter, the temperature is as low as -7 $^{\circ}\text{C}$ in the northern parts of the basin by both observed and NEX-GDDP ensemble. The range of mean temperature on all three averaging periods shows a very good agreement with the observations as compared to raw GCMs. The spatial biases of historical temperature are shown in Fig. 5. Both the higher magnitude and the large extent of bias (mostly cold) are evident for raw GCMs as compared to NEX-GDDP. Raw GCMs ensemble show very cold bias (more than 4 $^{\circ}\text{C}$) over most parts of KRB, except a few parts showing a warm bias (up to 3 $^{\circ}\text{C}$). In case of NEX-GDDP, there still exist noticeable differences with observation in terms of magnitude, but an overall improvement can be seen.

Skills of individual models (both raw GCMs and down-scaled NEX-GDDP) for the climatology of the seasonal cycle of basin-averaged precipitation over KRB is shown

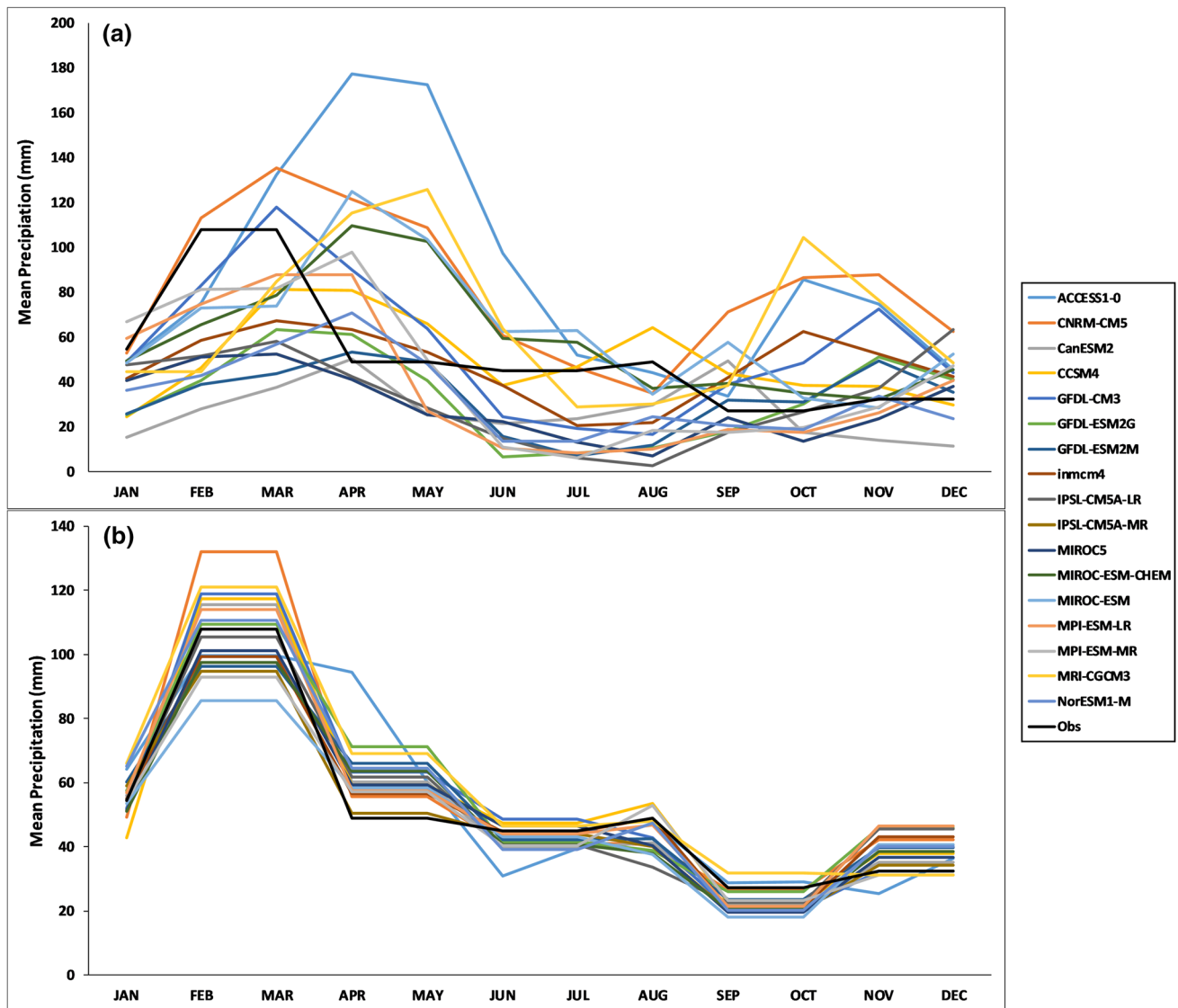


Fig. 6 Annual cycle of climatological mean basin-averaged precipitation (mm): **a** raw GCMs and **b** NEX-GDDP data set

in Fig. 6. It is obvious that raw GCMs exhibit quite varying skill (both underestimation/overestimation) and a large inter-model spread in simulating the observed precipitation (Fig. 6a). In Fig. 6b, the NEX-GDDP effectively corrects the relative bias in the seasonal cycle of all models and removes the inter-model spread of precipitation which was shown by raw GCMs (Fig. 6b). Therefore, all models of the NEX-GDDP data set are included in the multi-model ensemble to project future changes.

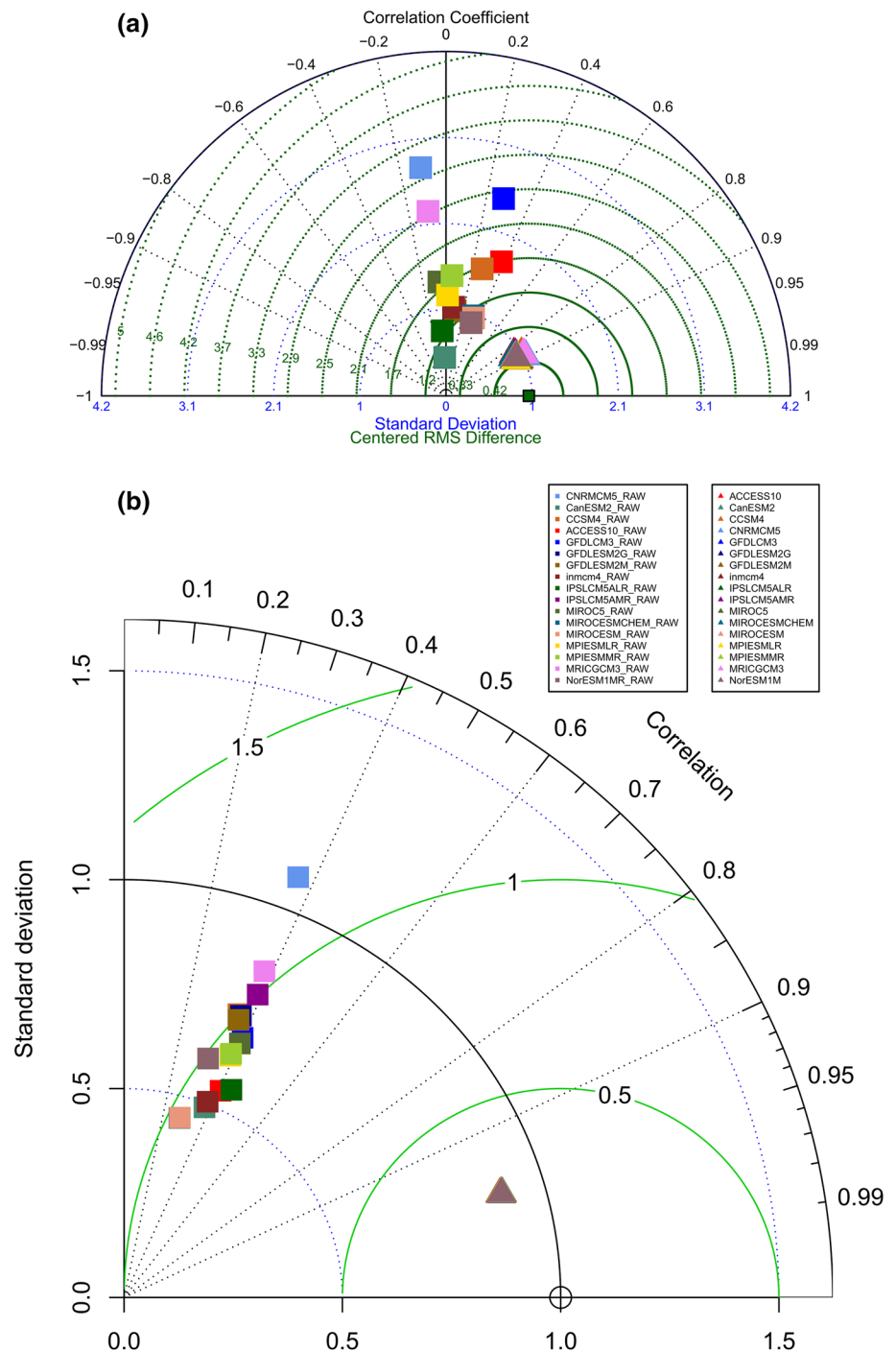
The Taylor diagram shows that all models of NEX-GDDP have a very high agreement with observations as compared to raw GCMs (Fig. 7). Not only are the inter-model agreement improved, but the individual models show a very good correlation coefficient with observation. The highly consistent statistics of temperature and precipitation produced by

NEX-GDDP can be attributed to bias correction and terrain-specific corrections. Since the same data set (GMFD) was used for the construction of bias-corrected NEX-GDDP data, the resulting models have a high agreement which is more evident in the case of temperature (Fig. 7b). Therefore, projections of temperature and precipitation based on NEX-GDDP tend to be more robust as compared to raw CMIP5 GCMs, particularly the downscaling technique employed resulted in the efficient representation of seasonal precipitation.

3.2 Future Climate Change

Figure 8 shows the ensemble-based median projected changes in temperature with respect to the historical period

Fig. 7 Taylor diagram based on monthly basin mean: **a** precipitation and **b** temperature for Kabul River Basin. Squares correspond to the raw GCMs, while triangles refer to NEX-GDDP data sets. Small square marks reference (observed) precipitation data set on x -axis, while observed temperature is marked by hollow circle on x -axis



under RCP4.5. On an annual basis, an increase of 1.5–1.8 °C is observed during near-term; an increase of 2.7–3 °C during mid-term; the highest rise of 3.2–3.7 °C by the EOC. During the JJAS, the future projections show an increase of 1.5–2.1 °C during near-term; 2.7–3.2 °C during mid-term and 3.2–3.7 °C during EOC. Similarly, an overall warming of 1.5–1.8 °C is shown during the DJFM near-term; 2.8–3.1 °C during mid-term and 3.5–4 °C during EOC. The warming appears more dominant in the western part of the

KRB for both annual and seasonal climatology. Increases in temperature are consistent with the previous findings of 2–4 °C over the same region (Wu et al. 2017). The projected rise in mean temperature is significant during 95% confidence level.

Figure 9 shows the median projected changes in precipitation for KRB under RCP4.5. A negative change in precipitation can be seen across the KRB during the twenty first century. The magnitude of the decrease is large during

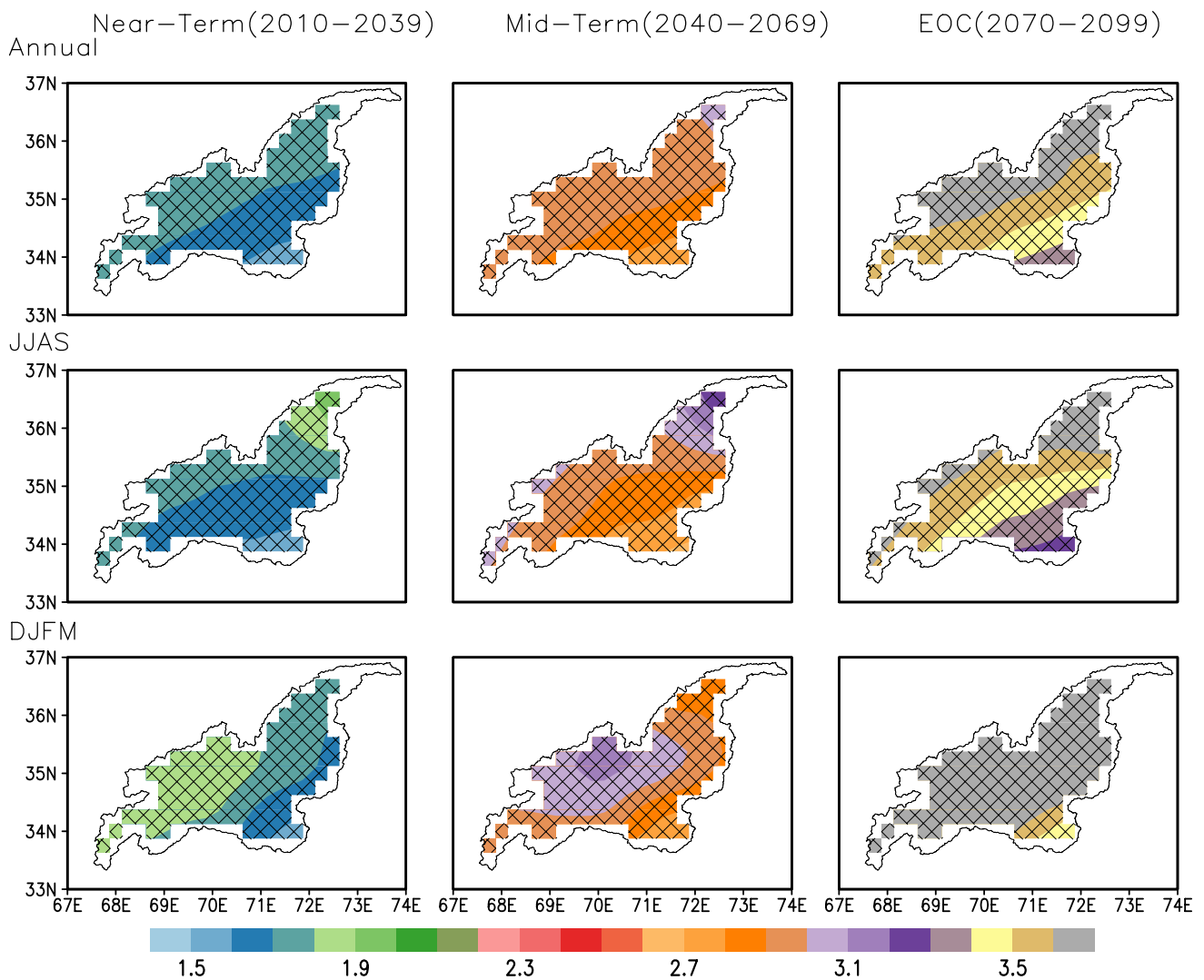


Fig. 8 Ensemble median projected changes in spatial distribution and magnitude of annual, summer (JJAS), and winter (DJFM) mean temperature (°C) for the periods 2010–2039, 2040–2069, and 2070–2099

under RCP4.5 with reference to the baseline period 1975–2005. The hatch represents significance at $\geq 95\%$ confidence level from a two-sample *t* test

DJFM, where a remarkable change can be seen during mid-term and EOC. The percentage of negative change is almost 50% and more across the KRB. During JJAS, there is spatial variation in terms of changes in precipitation from the west to east. The lower parts of the KRB, on the Pakistan side, show a slight decrease of around 20–30% while the western parts, mostly on the Afghanistan side, show a more negative change of around 50%. However, in contrast to temperature projections, the significant test does not indicate the robustness of these changes due to a disagreement of models for precipitation.

Figure 10 represents the climatology of projected median changes in temperature for the twenty first century under the RCP8.5 scenario. Annual average temperatures undergo an increase of 1.6–2 °C in the near-term over most parts of the basin and increase gradually towards the EOC as it

reaches up to 6.4 °C in the northern (snow-covered) region. It is observed that temperature change is much more drastic during DJFM, as compared to JJAS. The DJFM temperature rise starts from a range of 1.8–2 °C in the near-term and is projected to reach 5.8–6.8 °C by the EOC. The consistent increase in temperature until the end of the century is attributed to the fact that RCP8.5 is a continuous GHG emission rise scenario under which the radiative forcing will continue to feed the rising temperatures until the end of the century (Riahi et al. 2011). The projected warming is significant at a 95% confidence level on all climatic scales.

Figure 11 represents the projection of change in precipitation for three future periods (near-term, mid-term, and EOC), as compared to the historical precipitation under RCP8.5. Annual mean precipitation decreases slightly (–15 to 30%) over most parts of the domain during near-term. The

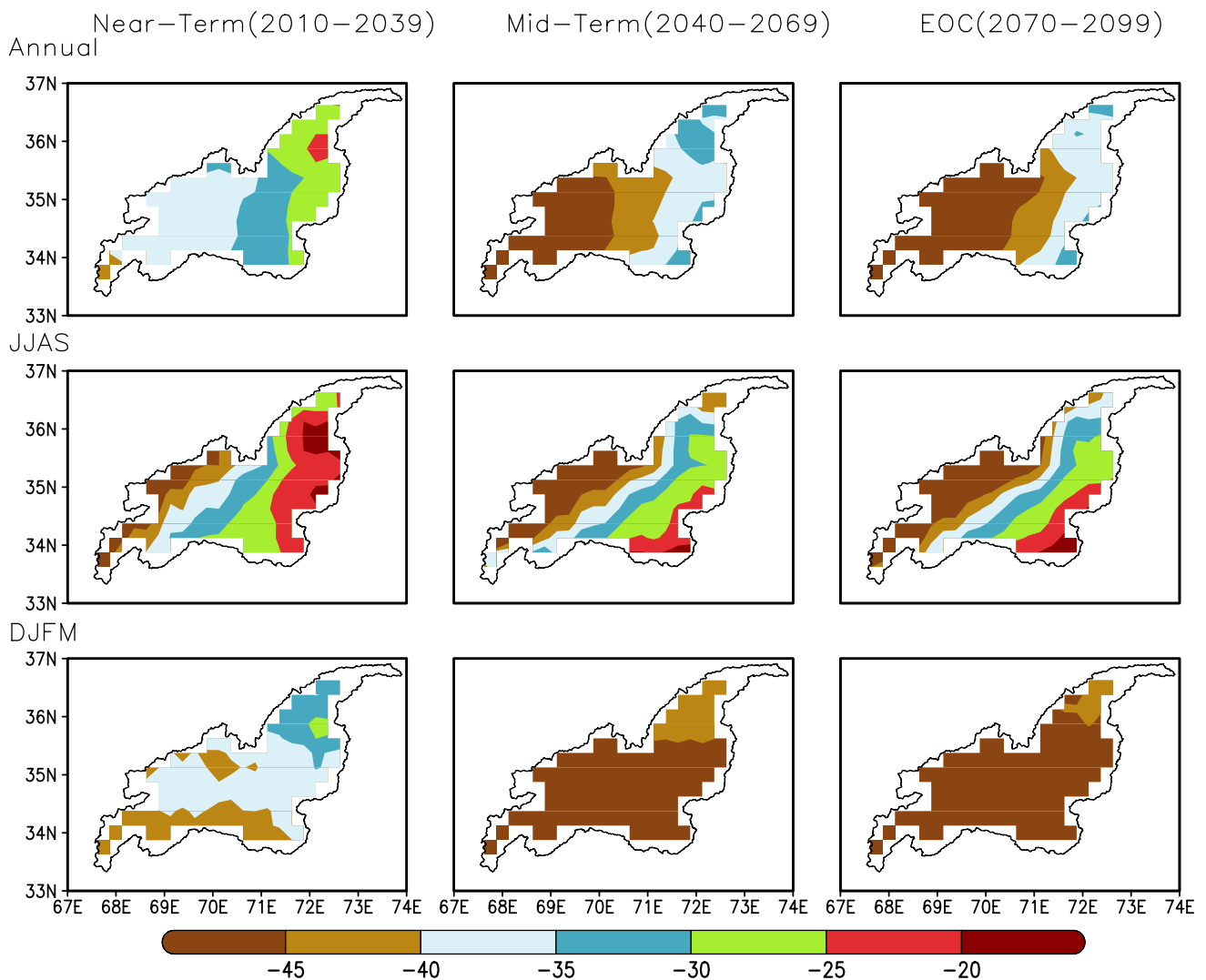


Fig. 9 Ensemble median projected changes in spatial distribution and magnitude of annual, summer (JJAS) and winter (DJFM) precipitation (%) for the periods 2010–2039, 2040–2069, and 2070–2099

under RCP4.5 with reference to the baseline period 1975–2005. The hatch represents significance at $\geq 95\%$ confidence level from a two-sample *t* test

increasing extent of a high negative change is seen towards the EOC with a decrease of more than 40%. JJAS projections indicate a slight change in precipitation (–5 to 20%) over most parts of KRB, while the lower parts (which are within the reach of monsoon) show a slight increase in precipitation (0–15%) by the EOC. DJFM precipitation is shown to decrease strongly towards the EOC where the whole region shows a decrease of more than 40%. However, the significance of these changes is not validated at a 95% confidence interval.

Figure 12a represents a frequency distribution of mean temperature averaged over the entire KRB for past and future periods during JJAS under the RCP4.5 scenario. The summer temperatures are projected to show warming in all future periods. The frequency distribution is negatively skewed, with more values shifting towards maximum

temperatures near the end of the century. The highest occurring temperature in the summer season is 19 °C (1975–2005) with an occurrence rate of around 1000 days. According to the projections, by the end of the twenty first century, this value would go up to as high as 24 °C with an occurrence rate of 800 days. Figure 12b represents a positively skewed distribution in DJFM, with temperature ranges from –5 to 14 °C. There is a significant shift in temperatures in all future projections as compared to the baseline. The maximum shift is found during 2070–2099, where temperatures vary from –1 to 14 °C compared to the baseline range of –5 to 9 °C.

Figure 12c shows a frequency distribution of annual average temperatures for baseline and future projections (RCP4.5). A shift towards more warming can be seen in future projections compared to the baseline. The baseline

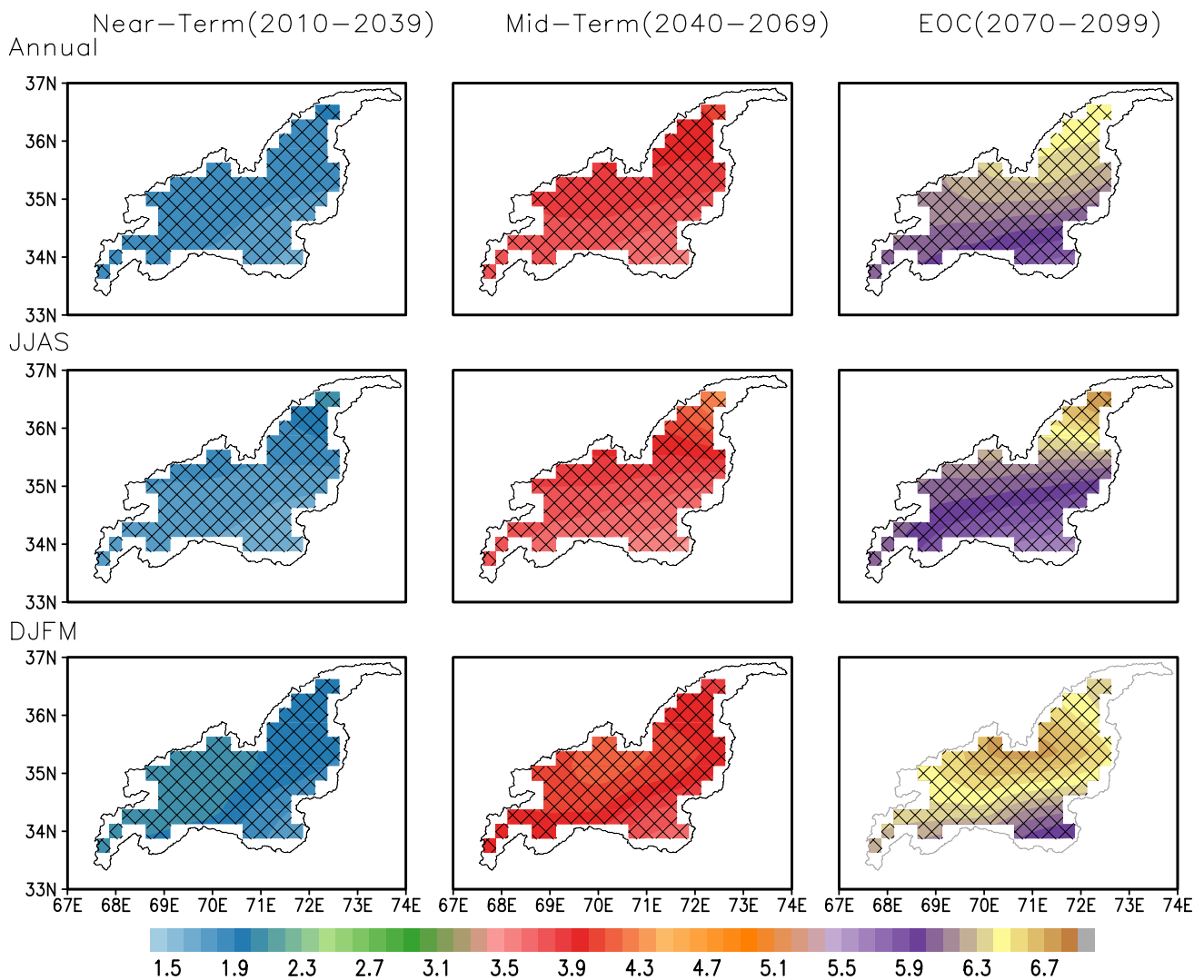


Fig. 10 Ensemble median projected changes in spatial distribution and magnitude of annual, summer (JJAS), and winter (DJFM) mean temperature (°C) for the periods 2010–2039, 2040–2069, and 2070–

2099 under RCP8.5 with reference to the baseline period 1975–2005. The hatch represents significance at $\geq 95\%$ confidence level from a two-sample *t* test

annual temperature varies from -5 to 21 °C, which shifts towards -1 to 24 °C towards the end of the century. The distribution is negatively skewed with a maximum occurrence (1000 days) observed for 24 °C at the end of the century. The value of kurtosis as represented in Table 2 is negatively increasing which can also be observed in Fig. 12c, which represents the concentration of data at the tail instead of the peak.

Figure 13a, b shows frequency distributions of precipitation for annual, JJAS, and DJFM, respectively, under the RCP4.5 scenario. Overall, both summer and winter precipitation are likely to decrease in future projections. The decrease in summer precipitation is more significant during near-term, whereas the frequency distribution remains almost the same during mid-term and EOC. Figure 13c represents the frequency distribution of daily precipitation

on an annual basis for baseline and future projections. A slight decrease in the frequency of precipitation events was observed in all future projections. The frequency distribution is positively skewed with most of the values between 0.5 and 4.5 mm/day. Similarly, Table 3 shows the summary characteristics of the frequency distribution curves. It shows maximum skewness during near-term and a maximum standard deviation (SD) during EOC, which means that extreme events are likely to increase by the end of the century.

Similar to Fig. 12, Fig. 14a represents the histogram for mean temperatures in JJAS. It follows a similar pattern as RCP4.5, with the highest frequency of 1000 days for a temperature value of 19 °C during 1975–2005. However, according to the projections, by the end of the twenty first century, this value would go up as high as 26 °C with an occurrence rate of 1000 days. Figure 14b represents a

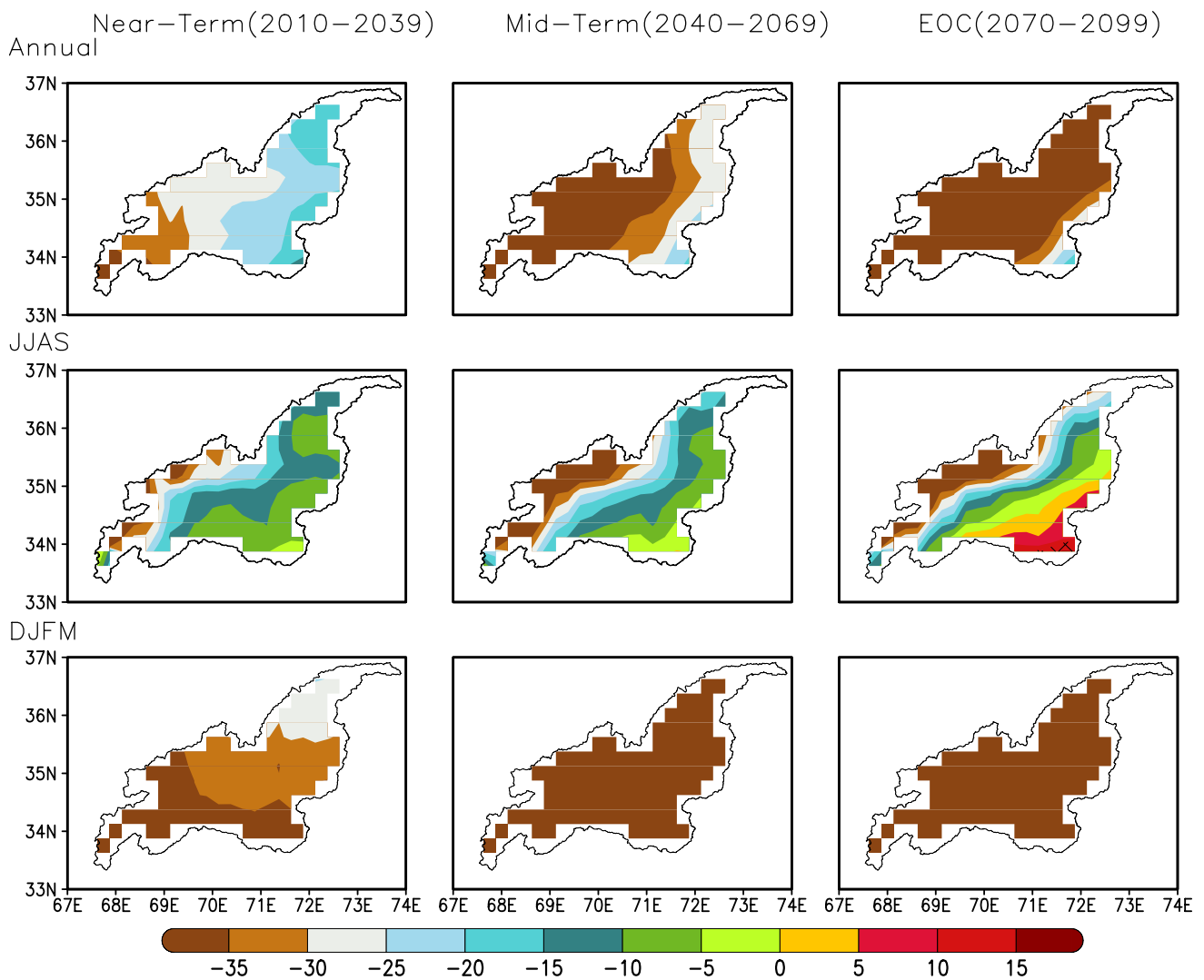


Fig. 11 Ensemble median projected changes in spatial distribution and magnitude of Annual, summer (JJAS), and winter (DJFM) precipitation (%) for the periods 2010–2039, 2040–2069, and 2070–2099

under RCP8.5 with reference to the baseline period 1975–2005. The hatch represents significance at $\geq 95\%$ confidence level from a two-sample *t* test

histogram of temperature for the DJFM. During the historical period (1975–2005), the highest occurrence (628 days) was observed for a mean temperature of -2°C . In the subsequent years, the occurrences of high mean temperatures have increased and, by the end of the century, the highest number of occurrences was observed at 5°C . For mean annual temperature (Fig. 14c), the visible shift in the frequency distributions of mean temperature can be seen, i.e., from -5 to 20°C during 1975–2005 to 5 – 26°C during EOC. The shift is evident from the values of skewness and kurtosis represented in Table 4. Figure 15a demonstrates the histogram of past and future precipitations during the summer season. Normal precipitation distribution lies from 0 to 5.5 mm/day during JJAS. However, in future periods, a decrease in the occurrence of high precipitation events is seen, although the tail of the distribution is slightly skewed

towards higher precipitation events in the future. During winter (Fig. 15b), no notable change in distribution can be observed. Figure 15c shows precipitation ranges from 0 to 8 mm/day on an annual basis during past and future periods. The highest number of occurrences for precipitation events lies between 0.8 and 3.2 mm/day. The right shift is attributed to the fact that the value of skewness increased negatively, whereas the negative values of kurtosis show that the data are concentrated at the tail of the distribution rather than at the peak. Unlike temperature, both annual and seasonal (JJAS and DJFM) precipitation remain positively skewed; the right tail is longer; the mass of the distribution is concentrated on the left. Table 5 represents the kurtosis, apart from the summer season, consistently increased, showing the concentration of data at the peaks and elongated tails due to an increase in skewness as well.

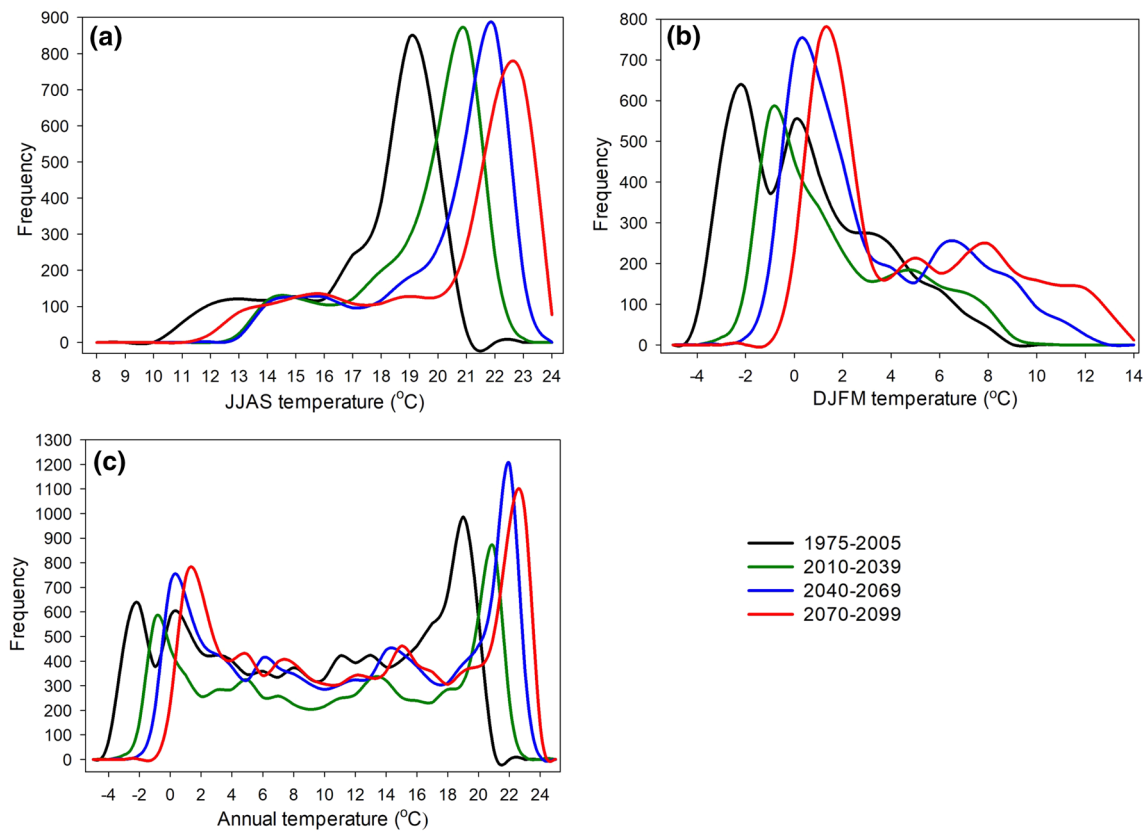


Fig. 12 Comparison of frequency distribution curve of **a** summer (JJAS), **b** winter (DJFM), and **c** annual temperature for future periods 2010–2039, 2040–2069, 2070–2099, and the baseline period 1975–2005 over the entire Kabul River Basin under RCP4.5

Table 2 Summary statistics of the frequency distribution of mean temperature (°C) for future periods 2010–2039, 2040–2069, 2070–2099, and the baseline period 1975–2005 under RCP 4.5

Year	Skew	Kurtosis	SD	Mean
Annual				
1975–2005	−0.08	−1.41	7.60	8.56
2010–2039	−0.08	−1.43	7.88	10.13
2040–2069	−0.09	−1.43	7.89	11.18
2070–2099	−0.06	−1.43	7.77	11.89
JJAS				
1975–2005	−1.17	0.29	2.43	17.13
2010–2039	−1.17	0.41	2.21	18.90
2040–2069	−1.16	0.23	2.52	19.60
2070–2099	−1.04	−0.23	3.14	19.82
DJFM				
1975–2005	0.60	−0.49	2.85	0.04
2010–2039	0.71	−0.62	2.89	1.24
2040–2069	0.74	−0.63	3.35	2.68
2070–2099	0.64	−0.89	3.81	4.15

4 Summary and Conclusions

NEX-GDDP is the most recent and up-to-date data set of statistically downscaled climate change projections that has benefited over raw CMIP5 GCMs in many aspects. Due to their coarse resolution, GCMs are not suited for catchment scale studies such as our study area; therefore, NEX-GDDP significantly overcomes this GCMs' limitation. Its high resolution provides valuable regional-scale information about climate change. Before looking into future changes in mean temperature and precipitation, a detailed investigation of NEX-GDDP evaluation against observations and CMIP5 raw GCMs is performed for the KRB. NEX-GDDP past climatology on an annual and seasonal basis is reasonably well matched with spatial features of the high-resolution observed data set. Taylor diagrams and seasonal cycles of NEX-GDDP-based models reveal very encouraging results in terms of the robustness and efficiency of these data in providing high-resolution regional climate change information. NEX-GDDP showed improved performance statistics

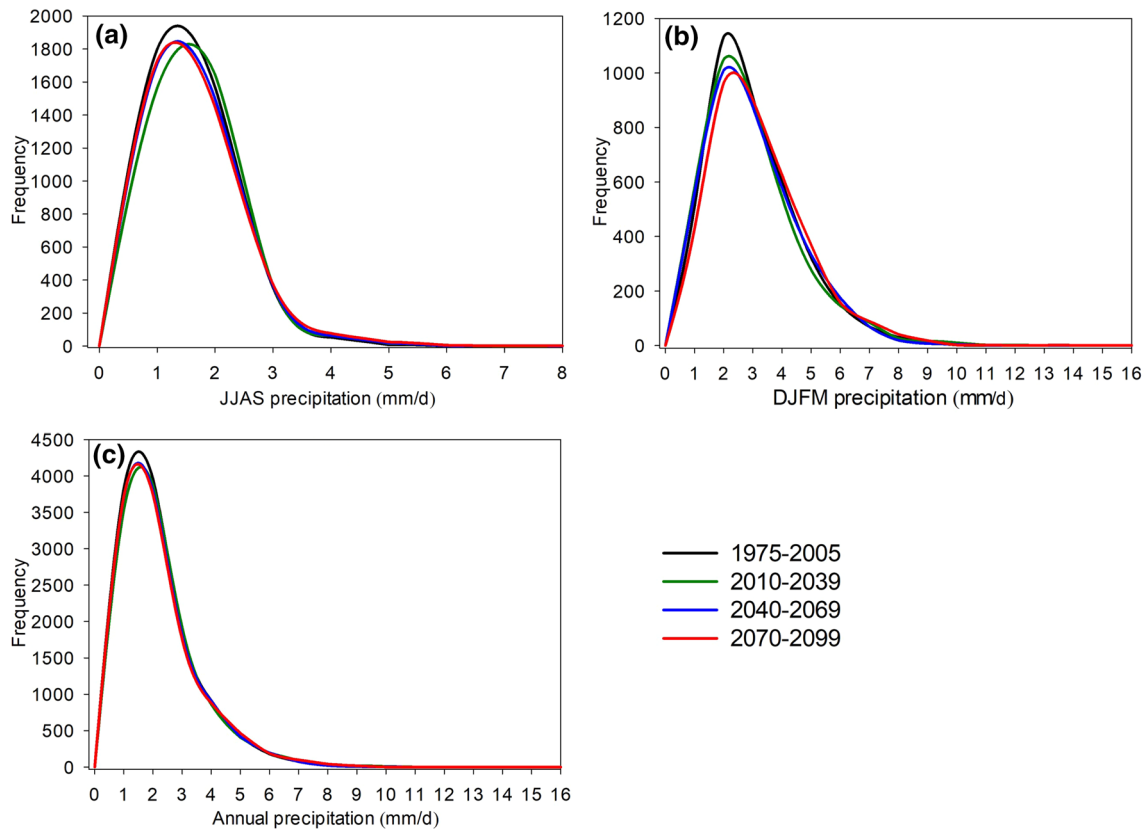


Fig. 13 Comparison of frequency distribution curve of **a** summer (JJAS), **b** winter (DJFM), and **c** annual precipitation (mm/day) for future periods 2010–2039, 2040–2069, 2070–2099, and the baseline period 1975–2005 over the entire Kabul River Basin under RCP4.5

Table 3 Summary statistics of the frequency distribution of precipitation (mm/day) for future periods 2010–2039, 2040–2069, 2070–2099, and the baseline period 1975–2005 under RCP 4.5

Year	Skew	Kurtosis	SD	Mean
Annual				
1975–2005	1.56	3.09	1.27	1.73
2010–2039	1.77	4.64	1.34	1.77
2040–2069	1.54	3.29	1.28	1.74
2070–2099	1.75	4.77	1.37	1.76
JJAS				
1975–2005	1.16	1.91	0.66	1.17
2010–2039	1.41	3.62	0.70	1.23
2040–2069	1.37	3.39	0.71	1.19
2070–2099	1.56	4.41	0.77	1.19
DJFM				
1975–2005	1.02	1.12	1.52	2.51
2010–2039	1.31	2.51	1.62	2.50
2040–2069	0.97	1.31	1.55	2.52
2070–2099	1.19	2.75	1.63	2.71

of historical climatology compared to CMIP5 raw GCMs in terms of reducing biases of monthly temperature and precipitation, particularly topography-related precipitation errors in GCMs, thus improving the accuracy and reliability of future projections. The multi-model ensemble of NEX-GDDP for the historical period (1975–2005) captures the spatial patterns of both temperature and precipitation in accordance with the observational data set. All three model performance evaluation statistics, i.e., the standard deviation (SD), Pearson's correlation, and root-mean-square difference (RMSD), are in agreement with the observed data. Bao and Wen (2017) drew a similar conclusion by evaluating NEX-GDDP and original GCMs against observations in China. They recommended the use of NEX-GDDP data sets for climate change studies at the local scale, owing to its performance in representing past extremes apart from means. Another study using NEX-GDDP was conducted by Chen et al. (2017) to evaluate the representation of historical precipitation extremes in China by NEX-GDDP data sets. Therefore, the projections of temperature and precipitation

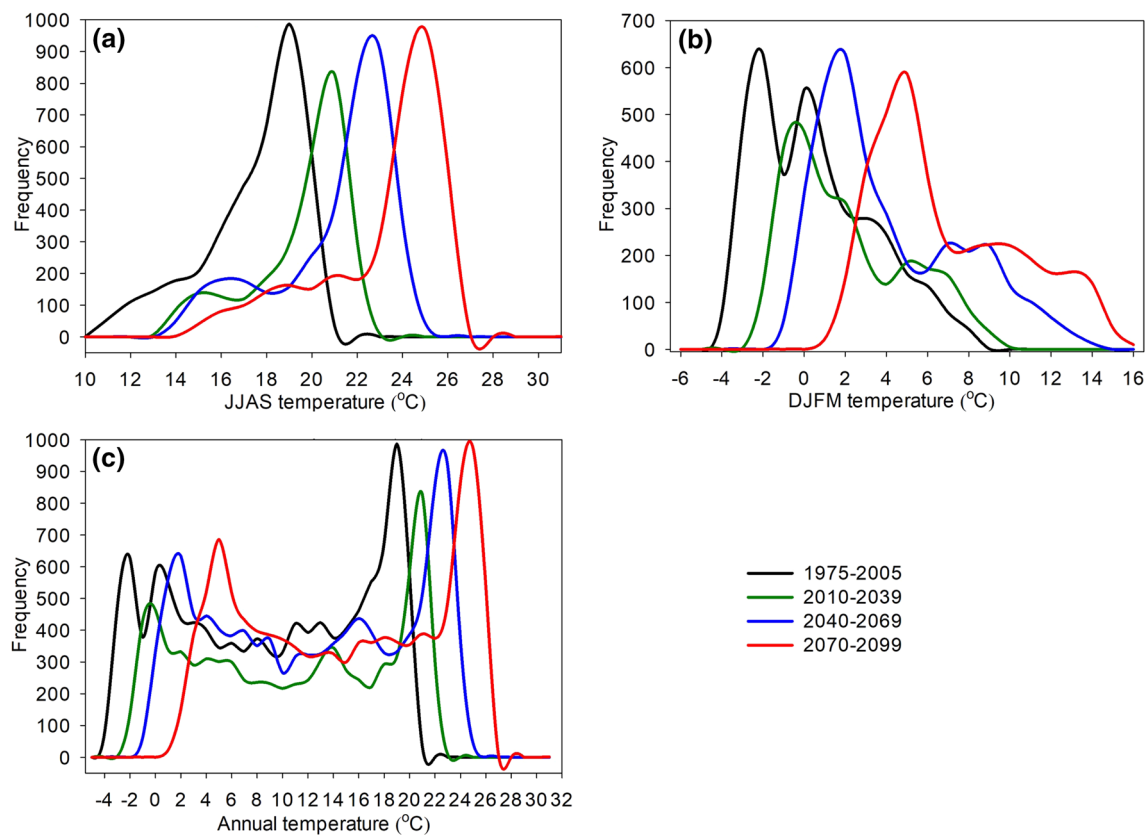


Fig. 14 Comparison of frequency distribution curve of **a** summer (JJAS), **b** winter (DJFM), and **c** annual temperature (°C) for future periods 2010–2039, 2040–2069, 2070–2099, and the baseline period 1975–2005 over the entire Kabul River Basin under RCP8.5

using NEX-GDDP data sets are comprehensive and at the finest scale and, when used with hydrological models, will

Table 4 Summary statistics of the frequency distribution of mean temperature (°C) for future periods 2010–2039, 2040–2069, 2070–2099, and the baseline period 1975–2005 under RCP 8.5

Year	Skew	Kurtosis	SD	Mean
Annual				
1975–2005	−0.08	−1.41	7.60	8.56
2010–2039	−0.08	−1.42	7.78	10.32
2040–2069	−0.08	−1.41	7.87	12.07
2070–2099	−0.09	−1.44	7.74	14.50
JJAS				
1975–2005	−1.00	0.26	2.24	16.96
2010–2039	−1.10	0.31	2.15	19.00
2040–2069	−1.03	0.02	2.64	20.53
2070–2099	−1.19	0.45	2.77	22.63
DJFM				
1975–2005	0.60	−0.48	2.84	0.03
2010–2039	0.63	−0.68	2.90	1.59
2040–2069	0.71	−0.56	3.50	3.69
2070–2099	0.60	−0.74	3.51	6.46

improve the understanding of future water resources available in the near-term and long-term under a changing climate.

Future projections of both mean temperature and precipitation are discussed for near-future, mid-term, and EOC. As seen from frequency distribution curves of the mean temperature, the shape is shifting rightward towards the end of the century with references to the historical period, indicating a warmer climate that could result in accelerated snow and glacier melt processes. However, it needs further investigations using hydrological modeling. With reference to past climates, future mean temperatures show a consistent rise in the future averaging period, particularly during mid-term and EOC for the entire KRB. However, high spatial variability exists in the thermal regime in the future. During the mid-century, the mean temperature may rise by 3.2 °C in the western parts of the domain under RCP4.5. Warming is further pronounced in the EOC (up to 3.7 °C) on both seasonal and annual basis. The rise in temperature is further enhanced when results under RCP8.5 scenario are analyzed. The range of temperature changes by the end of the century is 5.8–6.8 °C during DJFM. A noticeably enhanced warming can be seen for DJFM as compared to JJAS. The statistical

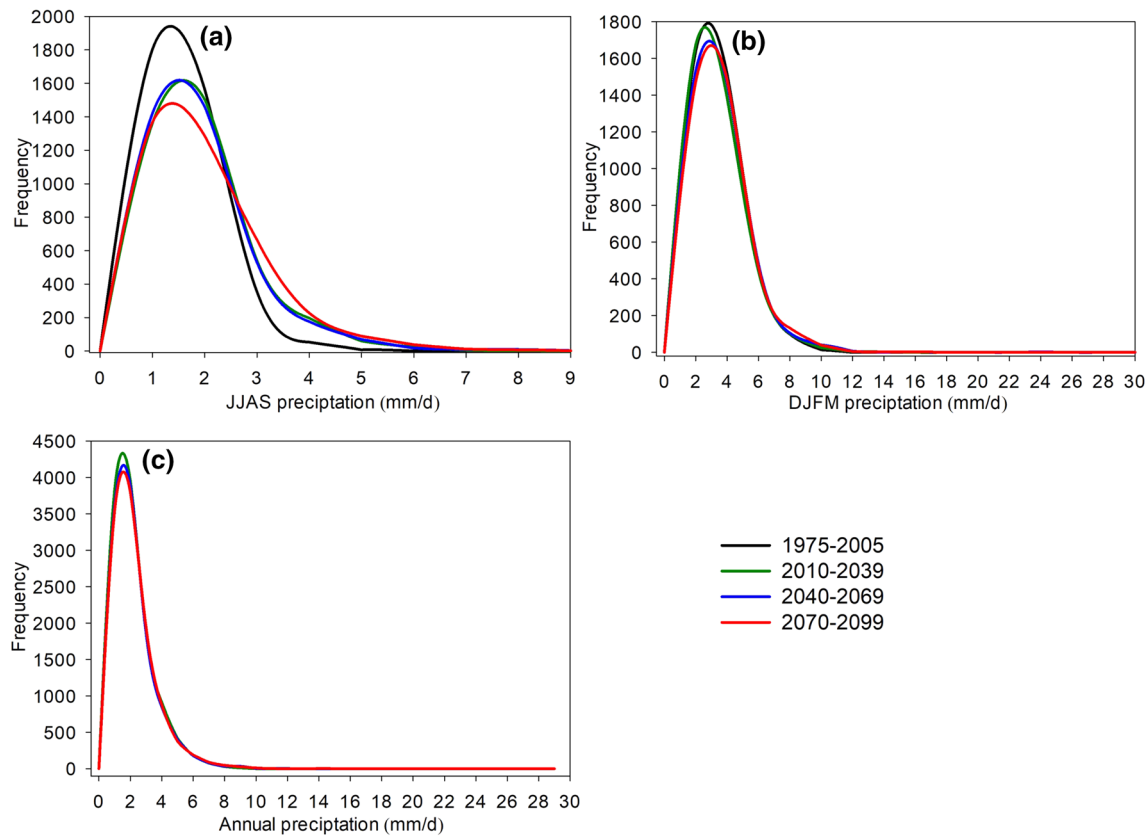


Fig. 15 Comparison of frequency distribution curve of **a** summer (JJAS), **b** winter (DJFM), and **c** annual precipitation (mm/day) for future periods 2010–2039, 2040–2069, 2070–2099, and the baseline period 1975–2005 over the entire Kabul River Basin under RCP8.5

significance of these changes is tested using student *t* test at a 95% confidence level.

Table 5 Summary statistics of the frequency distribution of precipitation for future periods 2010–2039, 2040–2069, 2070–2099, and the baseline period 1975–2005 under RCP 8.5

Year	Skew	Kurtosis	SD	Mean
Annual				
1975–2005	1.56	3.09	1.27	1.73
2010–2039	2.14	11.83	1.36	1.79
2040–2069	2.53	15.90	1.39	1.77
2070–2099	2.90	23.24	1.43	1.79
JJAS				
1975–2005	1.16	1.90	0.66	1.17
2010–2039	1.54	3.46	0.97	1.48
2040–2069	1.95	6.53	1.05	1.46
2070–2099	1.54	3.39	1.13	1.58
DJFM				
1975–2005	1.02	1.12	1.52	2.52
2010–2039	1.88	10.61	1.68	2.50
2040–2069	2.16	12.72	1.76	2.64
2070–2099	2.66	19.59	1.83	2.70

Projected changes in precipitation vary considerably in terms of both spatial variations and the magnitude of change. These variations are attributed to the presence of high elevation peaks and valleys in the domain, which result in an uneven distribution of precipitation across the basin under both emission scenarios. Under the RCP4.5 scenario, there is an evident decrease in twenty first century DJFM precipitation (up to 50% and more) across the KRB. During JJAS, the decrease in precipitation is more pronounced on the western parts of KRB in Afghanistan. Future precipitation under the RCP8.5 scenario shows a higher magnitude of precipitation decline as compared to RCP4.5. Summer precipitation is seen to decrease less compared to DJFM, while a slight positive change (0–15%) can also be seen in monsoon-approached parts of the KRB. Strong negative change signal, along with an increase in warming, may induce frequent occurrences of flash floods and affect stream flow dynamics. However, the hydrological responses to these climatic changes need to be simulated.

The results presented in this study provide a detailed estimation of future projections of temperature and precipitation in the KRB in relation to two emission scenarios. The information provided here can be used to further assess water resources using impact assessment models and can build a

knowledge base for policy making and adaptation efforts of both Pakistan and Afghanistan. However, the uncertainties associated with the use of multi-model ensembles and local topographic-based climate processes should be carefully considered when using these projections and feed them into a hydrological model.

Acknowledgements The National Academy of Sciences (NAS) and the United States Agency for International Development (USAID) Partnerships for Enhanced Engagement in Research (PEER) program supported this research under the project “Understanding our joint water-climate change challenge and exploring policy options for cooperation on the Afghan–Pak transboundary Kabul River Basin”. This project was developed and headed by Leadership for Environment and Development (LEAD) Pakistan, and implemented by Ms. Hina Lotia, Director Programmes, and Ms. Samar Minallah, Focal Person Water Programme, at LEAD Pakistan. Climate scenarios presented here were analyzed from the NEX-GDDP data set, prepared by the Climate Analytics Group and NASA Ames Research Center using the NASA Earth Exchange, and distributed by the NASA Center for Climate Simulation (NCCS). We also acknowledge CSIRO Land and Water, Australia, for providing observed gridded air temperature and precipitation data. We also want to thank Mr. Khalid Mohtadullah who provided valuable insight and expertise that assisted in improving the manuscript. We are also grateful to reviewers for the positive criticism and suggestions that have provided a better insight into the scientific delivery of the topic.

Compliance with Ethical Standards

Conflict of interest On behalf of all authors, the corresponding author states that there is no conflict of interest.

References

- Abbaspour K (2015) SWAT-CUP (2015) SWAT calibration and uncertainty programs—a user manual; EAWAG. Swiss Federal Institute of Aquatic Science and Technology, Zurich
- Almazroui M, Abid M, Athar H, Islam M, Ehsan M (2012) Interannual variability of rainfall over the Arabian Peninsula using the IPCC AR4 Global Climate Models. *Int J Climatol* 33(10):2328–2340
- Annamalai H, Hamilton K, Sperber K (2007) The South Asian summer monsoon and its relationship with ENSO in the IPCC AR4 simulations. *J Clim* 20(6):1071–1092
- Bachner S, Kapala A, Simmer C (2008) Evaluation of daily precipitation characteristics in the CLM and their sensitivity to parameterizations. *Meteorol Z* 17(4):407–419
- Bajracharya SR, Shrestha B (eds) (2011) The status of glaciers in the Hindu Kush–Himalayan region. ICIMOD, Kathmandu
- Bao Y, Wen X (2017) Projection of China’s near-and long-term climate in a new high-resolution daily downscaled dataset NEX-GDDP. *J Meteorol Res* 31(1):236–249. <https://doi.org/10.1007/13351-017-6106-6>
- Chen YJ, Shui K, Shi H, Zheng (2016) Analysis of historical climate datasets for hydrological modelling across south Asia. CSIRO Sustainable Development Investment Portfolio Project. Technical report. CSIRO Land and Water, Acton
- Chen HP, Sun JQ, Li HX (2017) Future changes in precipitation extremes over China using the NEX-GDDP high-resolution daily downscaled data-set. *Atmos Ocean Sci Lett* 10:403–410
- Cruz RVH, Change Climate et al (2007) Impacts, adaptation and vulnerability. Contribution of Working Group II to the Fourth Assessment Report of the Intergovernmental Panel on Climate Change. Cambridge University Press, Cambridge, pp 469–506
- Ekström M, Grose MR, Whetton PH (2015) An appraisal of downscaling methods used in climate change research. *Wiley Interdiscip Rev Clim Change* 6(3):301–319
- FAO (2016) Land cover atlas of The Islamic Republic of Afghanistan. <http://www.fao.org/3/a-i5457e.pdf>. Accessed 19 July 2018
- Ficklin DL, Abatzoglou JT, Robeson SM, Dufficy A (2016) The influence of climate model biases on projections of aridity and drought. *J Clim* 29(4):1269–1285
- Giorgi F, Coppola E, Solmon F, Mariotti L, Sylla MB, Bi X, Elguindi N, Diro GT, Nair V, Giuliani G, Turuncoglu UU (2012) RegCM4: model description and preliminary tests over multiple CORDEX domains. *Clim Res* 52:7–29
- Hassanyar MH, Hassani S, Dozier J (2017) Multi-model ensemble climate change projection for Kabul River Basin, Afghanistan under representative concentration pathways. *Glob Res Dev J Eng* 02(05):69–78
- Hasson S, Lucarini V, Pascale S (2013) Hydrological cycle over south and southeast Asian river basins as simulated by PCMDI/CMIP3 experiments. *Earth Syst Dyn Discuss* 4(1):109–177
- Hasson S, Pascale S, Lucarini V, Böhner J (2016) Seasonal cycle of precipitation over major river basins in South and Southeast Asia: a review of the CMIP5 climate models data for present climate and future climate projections. *Atmos Res* 180:42–63
- Hasson S, Böhner J, Chishtie F (2018) Low fidelity of CORDEX and their driving experiments indicates future climatic uncertainty over Himalayan watersheds of Indus basin. *Clim Dyn*. <https://doi.org/10.1007/s00382-018-4160-0>
- Hutchinson MF, Xu T (2013) Anusplin version 4.4 user guide: fenner school of environment and society canberra, Australia. <http://fenner.school.anu.edu.au/files/anusplin44.pdf>. Accessed 19 July 2018
- Immerzeel WW, Van Beek LPH, Konz M, Shrestha AB, Bierkens MFP (2012) Hydrological response to climate change in a glacierized catchment in the Himalayas. *Clim Change* 110(3–4):721–736
- Iqbal W, Syed FS, Sajjad H, Nikulin G, Kjellström E, Hannachi A (2016) Mean climate and representation of jet streams in the CORDEX South Asia simulations by the regional climate model RCA4. *Theoret Appl Climatol*. <https://doi.org/10.1007/s00704-016-1755-4>
- Iqbal M, Dahri Z, Querner E, Khan A, Hofstra N (2018) Impact of climate change on flood frequency and intensity in the Kabul River Basin. *Geosci* 8(4):114
- Jarvis AHI, Reuter A, Nelson E, Guevara (2008) Hole-filled SRTM for the globe version 4, available from the CGIAR-CSI SRTM 90 m Database. <http://srtm.csi.cgiar.org>. Accessed 01 Jan 2018
- Jianchu X, Arun S, Rameshananda V, Mats E, Kenneth H (2007) The melting Himalayas. In: Regional challenges and local impacts of climate change on mountain ecosystems and livelihoods, ICIMOD Technical Paper, Kathmandu, p 2
- King M, Sturtewagen B (2010) Making the most of Afghanistan’s river basins: Opportunities for regional cooperation. EastWest Institute, New York
- Knutti R (2008) Should we believe model predictions of future climate change? *Philos Trans R Soc Lond A Math Phys Eng Sci* 366(1885):4647–4664
- Lashkaripour G, Hussaini S (2007) Water resource management in Kabul river basin, eastern Afghanistan. *Environmentalist* 28(3):253–260
- Leung LR, Mearns LO, Giorgi F, Wilby RL (2003) Regional climate research: needs and opportunities. *Bull Am Meteorol Soc* 84(1):89–95
- Lutz AF, ter-Maat HW, Biemans H, Shrestha AB, Wester P, Immerzeel WW (2016) Selecting representative climate models for climate change impact studies: an advanced envelope based selection approach. *Int J Climatol* 36(12):3988–4005

- Madadgar S, Moradkhani H (2014) Improved Bayesian multimodeling: integration of copulas and Bayesian model averaging. *Water Resour Res* 50(12):9586–9603
- Maurer EP, Hidalgo HG (2008) Utility of daily vs. monthly large-scale climate data: an intercomparison of two statistical downscaling methods. *Hydrol Earth Syst Sci Discuss* 12:551–563
- Mehmood S, Muhammad AA, Faisal SS, Muhammad MS, Arshad MK (2009) Climate change projections over South Asia under SRES A2 scenario using regional climate model RegCM3. https://www.researchgate.net/publication/284367455_Climate_Change_Projections_over_South_Asia_under_SRES_A2_Scenario_using_Regional_Climate_Model_RegCM3. Accessed 19 July 2018
- Meinshausen M, Smith SJ, Calvin K, Daniel JS, Kainuma MLT, Lamarque JF, Matsumoto K, Montzka SA, Raper SCB, Riahi K, Thomson AGJM (2011) The RCP greenhouse gas concentrations and their extensions from 1765 to 2300. *Clim Change* 109(1–2):213
- Murphy J (1999) An evaluation of statistical and dynamical techniques for downscaling local climate. *J. Climate* 12(8):2256–2284
- Nestler A, Huss M, Ambartzumian R, Hambarian A (2014) Hydrological implications of covering wind-blown snow accumulations with geotextiles on Mount Aragats, Armenia. *Geosciences* 4(3):73–92
- Pal JS, Giorgi F, Bi X, Elguindi N, Solmon F, Rauscher SA, Gao X, Francisco R, Zakey A, Winter J, Ashfaq M (2007) Regional climate modeling for the developing world: the ICTP RegCM3 and RegCM3. *Bull Am Meteorol Soc* 88(9):1395–1409
- Palazzi E, Hardenberg JV, Provenzale A (2013) Precipitation in the Hindu-Kush Karakoram Himalaya: observations and future scenarios. *J Geophys Res Atmos* 118(1):85–100
- Palazzi E, von-Hardenberg J, Terzago S, Provenzale A (2015) Precipitation in the Karakoram–Himalaya: a CMIP5 view. *Clim Dyn* 45(1–2):21–45
- Parajka J, Dadson S, Lafon T, Essery R (2010) Evaluation of snow cover and depth simulated by a land surface model using detailed regional snow observations from Austria. *J Geophys Res Atmos* 115(D24):17. <https://doi.org/10.1029/2010JD014086>
- Pfeiffer A, Zängl G (2011) Regional climate simulations for the European Alpine Region—sensitivity of precipitation to large-scale flow conditions of driving input data. *Theor Appl Climatol* 105(3–4):325–340
- Rajbhandari R, Shrestha A, Kulkarni A, Patwardhan S, Bajracharya S (2015) Projected changes in climate over the Indus river basin using a high-resolution regional climate model (PRECIS). *Clim Dyn* 44(1–2):339–357
- Riahi K, Rao S, Krey V, Cho C, Chirkov V, Fischer G, Kindermann G, Nakicenovic N, Rafaj P (2011) RCP 8.5—a scenario of comparatively high greenhouse gas emissions. *Clim Change* 109(1–2):33–57
- Rummukainen M (2010) State of the art with regional climate models. *Wiley Interdiscip Rev Clim Change* 1(1):82–96. <https://doi.org/10.1002/wcc.8>
- Sheffield J, Goteti G, Wood EF (2006) Development of a 50-year high-resolution global dataset of meteorological forcings for land surface modeling. *J Clim* 19(13):3088–3111
- Sidiqi M, Shrestha S, Ninsawat S (2018) Projection of climate change scenarios in the Kabul River Basin, Afghanistan. *Curr Sci* 114(06):1304
- Singh SP, Bassignana-Khadka I, Singh KB, Sharma E (2011) Climate change in the Hindu Kush–Himalayas: the state of current knowledge. International centre for integrated mountain development (ICIMOD). http://lib.icimod.org/record/9417/files/icimod-climate_change_in_the_hindu_kush-himalayas.pdf. Accessed 19 July 2018
- Su B, Huang J, Gemmer M, Jian D, Tao H, Jiang T, Zhao C (2016) Statistical downscaling of CMIP5 multi-model ensemble for projected changes of climate in the Indus River Basin. *Atmos Res* 178:138–149
- Suzuki-Parker A (2012) Uncertainties and limitations in simulating tropical cyclones. Springer Science & Business Media, Berlin
- Syed FS, Iqbal W, Syed AAB, Rasul G (2014) Uncertainties in the regional climate models simulations of South-Asian summer monsoon and climate change. *Clim Dyn* 42(7–8):2079–2097
- Syed FS, Shahbaz MM, Adnan A, M MS, Arshad MK (2009) Validation of the regional climate model RegCM3 over South Asia. https://www.researchgate.net/publication/284367453_Validation_of_the_Regional_Climate_Model_RegCM3_over_South_Asia/citations. Accessed 19 July 2018
- Taylor K (2001) Summarizing multiple aspects of model performance in a single diagram. *J Geophys Res Atmos* 106(D7):7183–7192
- Taylor KE, Stouffer RJ, Meehl GA (2012) An overview of CMIP5 and the experiment design. *Bull Am Meteorol Soc* 93(4):485–498. <https://doi.org/10.1175/BAMS-D-11-00094.1>
- Tebaldi C, Knutti R (2007) The use of the multi-model ensemble in probabilistic climate projections. *Philos Trans R Soc Lond A Math Phys Eng Sci* 365(1857):2053–2075
- Thrasher B, Maurer EP, McKellar C, Duffy PB (2012) Bias correcting climate model simulated daily temperature extremes with quantile mapping. *Hydrol Earth Syst Sci* 16(9):3309–3314
- Thrasher B, Xiong J, Wang W, Melton F, Michaelis A, Nemani R (2013) Downscaled climate projections suitable for resource management. *Eos Trans Am Geophys Union* 94(37):321–323
- UNFPA. A socio-economic and demographic profile - Afghanistan agriculture. UNFPA, Kabul, pp 2–3 (n.d.). <https://afghanag.ucdavis.edu/country-info/files/all-Afghanistan.pdf>. Accessed 19 July 2018
- Vidale PL, Lüthi D, Frei C, Seneviratne SI, Schär C (2003) Predictability and uncertainty in a regional climate model. *J Geophys Res Atmos*. <https://doi.org/10.1029/2002JD002810>
- Wilby RL, Charles SP, Zorita E, Timbal B, Whetton P, Mearns LO (2004) Guidelines for use of climate scenarios developed from statistical downscaling methods. In: Supporting material of the intergovernmental panel on climate change, available from the DDC of IPCC TGCA, p 27. http://www.ipcc-data.org/guidelines/dgm_no2_v1_09_2004.pdf. Accessed 19 July 2018
- Wood AW, Maurer EP, Kumar A, Lettenmaier DP (2002) Long range experimental hydrologic forecasting for the eastern United States. *J Geophys Res Atmos*. <https://doi.org/10.1029/2001JD000659>
- Wood AW, Leung LR, Sridhar V, Lettenmaier DP (2004) Hydrologic implications of dynamical and statistical approaches to downscaling climate model outputs. *Clim Change* 62(1):189–216
- Wu J, Xu Y, Gao XJ (2017) Projected changes in mean and extreme climates over Hindu Kush Himalayan region by 21 CMIP5 models. *Adv Clim Change Res* 8:176–184. <https://doi.org/10.1016/j.accre.2017.03.001>
- Yadav R, Yoo J, Kucharski F, Abid M (2010) Why is ENSO influencing northwest India decades? *J Clim* 23(8):1979–1993



Mr. Syed Ahsan Ali Bokhari is affiliated with the Pakistan Meteorological Department as a research engineer. His research interests include high performance computing, numerical weather prediction and regional climate modelling. He did his undergraduate in Electronic Engineering from International Islamic University, while he did masters in Climate Change Science and Policy from the University of Bristol, United Kingdom with distinction. He was also awarded the “Outstanding

Research Performance Prize” for his dissertation on wind power potential in the UK under Climate Change. He has worked on several local and international collaborative research projects related to climate change modeling.



Mr. Burhan Ahmad's main scientific expertise is associated with the use of gridded datasets to understand climate dynamics and extreme indices. He received his Master's degree in 2016 from COMSATS Institute of Information Technology with compulsory thesis work on modeling of Probability Density Functions for analyzing climate change. Mr. Burhan has supervised several graduate and postgraduate students from reputed universities. Besides that, he has professional experience of working in

climate modeling and downscaling with GISS NASA, RIMES, NCC, CAS, ICIMOD and CSIRO. He has worked on several research projects focused on agricultural, hydrological and climate modeling. Regarding academic research, he has ten research publications and three books on climate change.



Jahangir Ali is working as Research Assistant at Leadership for Environment and Development (LEAD) Pakistan. His special interests are climate change modelling and water resources management. He has received his Master's degree in Water Resources Engineering & Management and Bachelor's degree in Civil Engineering from the National University of Sciences and Technology (NUST).



Mr. Shakeel Ahmad earned his Master Degree in Environmental Sciences from COMSATS Institute of Information Technology, Pakistan, in 2017. Currently, he is enrolled as a Ph.D student at the School of Environment, Tsinghua University, China. Besides this, he worked as a Research Assistant at LEAD Pakistan with collaboration of Pakistan Meteorological Department Islamabad, Pakistan. Previously he worked as a Research Assistant at COMSATS Institute of

Information Technology. His research interests are cryosphere, climate change, hydrology and remote sensing.



Mr. Haris Mushtaq earned his Master's degree in Energy Systems Engineering from the National University of Sciences and Technology (NUST). He is currently working as a research associated with LEAD Pakistan. He has worked with Oregon State University as a research scholar where he conducted a research project analyzing Gravity Recovery and Climate Experiment (GRACE) data for terrestrial water mass over ten years' time in the Northern Pakistan region to investigate long term

trends of water mass.



Dr. Ghulam Rasul is a well-known scientist and a researcher in the field of Atmospheric Sciences and Climate Change who has more than 100 publications and research articles in National and International journals. He has vast experience in the field of agro-meteorology, meteorology, glaciology and climatology. He was awarded by SAARC Young Scientists Award in 1993 and won Senior Scientist Research Award in 2007. He is also working as a Coordinator of Climate Services Group in World Meteorological Organization (WMO), Co-Chair of Asian Water Cycle Initiative (AWCI) of Global earth Observation Systems (GEOS), Member of World Bank's Abu Dhabi Dialogue for Indus Basin, Member of Integrated Research on Disaster Risk Reduction (IDRR) of UNISDR and Vice-Chair, Academic Committee of Asia-Europe Meeting (ASEM) on Climate and Weather.

ological Organization (WMO), Co-Chair of Asian Water Cycle Initiative (AWCI) of Global earth Observation Systems (GEOS), Member of World Bank's Abu Dhabi Dialogue for Indus Basin, Member of Integrated Research on Disaster Risk Reduction (IDRR) of UNISDR and Vice-Chair, Academic Committee of Asia-Europe Meeting (ASEM) on Climate and Weather.